**Salinity gradient energy generation by pressure retarded osmosis: A review**

Ralph Rolly Gonzales [a], Ahmed Abdel-Wahab [b], Samer Adham [c], Dong Suk Han [d], Sherub Phuntsho [a], Wafa Suwaileh [e], Nidal Hilal [f], Ho Kyong Shon [a*]

[a] *Centre for Technology in Water and Wastewater, University of Technology Sydney, Ultimo, New South Wales, Australia*

[b] *Chemical Engineering Program, Texas A & M University at Qatar, Education City, Doha, Qatar*

[c] *Global Water Sustainability Center, Conoco Phillips, Qatar Science & Technology Park, Doha, Qatar*

[d] *Center for Advanced Materials, Qatar University, Doha, Qatar*

[e] *Qatar Foundation Research and Development, Qatar Foundation, Doha, Qatar*

[f] *NUAD Water Research Center, New York University Abu Dhabi, United Arab Emirates*

* Corresponding author; Email: hokyong.shon-1@uts.edu.au

**Abstract**

Pressure retarded osmosis (PRO) has gained attention due to its use as a salinity gradient energy-generating membrane process. This process can convert difference in salinity between two streams into energy as it allows water transport through a semi-permeable membrane against the application of hydraulic pressure. This review provides a comprehensive look at the history and latest developments in preparation of membranes and modules for the PRO process, as well as the various applications of PRO. This review also explored the influence of feed characteristics and pretreatment strategies on water permeation and power generation during PRO operation. The current status and technological advancements of PRO as a process were reviewed, revealing how PRO can be operated as a stand-alone process or in integration with other hybrid processes. Despite the recent advancements in material and process development for PRO, membrane performance, wide-scale implementation, and commercialization efforts still leave much to be desired. Recognizing the current challenges facing the PRO technology, the advancements in PRO membrane and module development, and the various applications of the process, this review also draws out the future direction of PRO research and generation of osmotic salinity gradient energy as a viable energy source.

**Highlights**

1. Various membrane and module development methods were comprehensively reviewed.
2. Dual-stage PRO process is promising for power generation over individual PRO process.
3. Novel configurations and niche applications of PRO can further be exploited.
4. Challenges and future recommendations for improving PRO process are discussed.

**Keywords:**

Pressure retarded osmosis; Engineered osmosis; Salinity gradient energy; Membrane; Osmotic energy

**List of abbreviations**

| Abbreviation | Meaning |
|---|---|
| RED | Reverse electrodialysis |
| CapMix | Capacitive mixing |
| BattMix | Battery mixing |
| PRO | Pressure retarded osmosis |
| FS | Feed solution |
| DS | Draw solution |
| W | Power density |
| RSF | Reverse solute flux |
| CP | Concentration polarization |
| ICP | Internal concentration polarization |
| ECP | External concentration polarization |
| RO | Reverse osmosis |
| CA | Cellulose acetate |
| CTA | Cellulose triacetate |
| HTI | Hydration Technologies Inc. |
| TFC | Thin film composite |
| NIPS | Nonsolvent-induced phase separation |
| PA | Polyamide |
| MPD | *m*-Phenylenediamine |
| TMC | Trimesoyl chloride |
| PSf | Polysulfone |
| PET | Polyethylene terephthalate |
| PEi | Polyetherimide |
| PVP | Polyvinylpyrrolidone |
| PAN | Polyacrylonitrile |
| CNT | Carbon nanotube |
| PES | Polyethersulfone |
| GO | Graphene oxide |
| HNT | Halloysite nanotube |
| COF | Covalent organic framework |
| TFN | Thin film nanocomposite |
| SNW-1 | Melamine-based Schiff base network |
| PE | Polyethylene |
| PVA | Polyvinyl alcohol |

| | |
|---|---|
| GA | Glutaraldehyde |
| TIPS | Thermal induced phase separation |
| PDA | Polydopamine |
| TBP | Tributylphosphate |
| BTDA-TDI-MDI | Copolymer of 3,3',4,4'-benzophenone tetra-carboxylic dianhydride and 80% methylphenylenediamine and 20% methylene diamine |
| PBI | Polybenzimidazole |
| POSS | Polyhedral oligomeric silsesquioxane |
| DI water | Deionized water |
| HPG | Hyperbranched polyglycerol |
| APTMS | 3-Aminopropyltrimethoxysilane |
| MPC | Zwitterionic 2-methacryloyloxyethylphosphorylcholine |
| AEMA | 2-Aminoethyl methacrylate hydrochloride |
| PAH | Poly(allylamine hydrochloride) |
| LBL | Layer by layer |
| GA | Glutaraldehyde |
| CQDs | Carbon quantum dots |
| T-NIPS | Thermally-assisted nonsolvent-induced phase separation |
| PP-$HSO_3$ | Sulfonate-functionalized porous polymer |
| TEOS | Tetraethyl orthosilicate |
| PEI | Polyethyleneimine |
| IPC | Isophthaloyl chloride |
| SWRO | Seawater reverse osmosis |
| MD | Membrane distillation |
| VMD | Vacuum membrane distillation |
| NF | Nanofiltration |
| MBR | Membrane bioreactor |
| LIS | Liquid-phase ion-stripping |
| OHE | Closed-loop osmotic heat engine |
| $NH_4HCO_3$ | Ammonia-carbon dioxide |
| MED | Multi-effect distillation |
| NOM | Natural organic matter |
| TOC | Total organic carbon |
| UF | Ultrafiltration |
| LP-RO | Low-pressure reverse osmosis |
| EDTA | Ethylenediaminetetraacetic acid |
| AL-FS | Active layer facing the feed solution |

| | |
|---|---|
| AL-DS | Active layer facing the draw solution |
| CDCF | Dual-stage PRO process with continuous draw and feed |
| DDCF | Dual-stage PRO process with divided draw and continuous feed |
| CDDF | Dual-stage PRO process with continuous draw and divided feed |
| DDDF | Dual-stage PRO process with divided draw and feed |

**List of symbols**

| Symbol | Meaning |
|---|---|
| $\Delta G_{mix}$ | Gibbs free energy of mixing |
| $G_B$ | Gibbs free energy of brackish water |
| $G_F$ | Gibbs free energy of fresh water |
| $G_S$ | Gibbs free energy of salt water |
| $\Delta H_{mix}$ | Enthalpy of mixing |
| $\Delta S_{mix}$ | Total molar entropy |
| $T$ | Absolute temperature |
| $R$ | Gas constant |
| $a_s$ | Activity coefficient of the product solution |
| $ns$ | Number of moles of the product solution |
| $\pi ss$ | Osmotic pressure of the salty solution |
| $\bar{V}_s$ | Molar volume of the final solution |
| $n_M$ | Moles of ions in a mixture |
| $n_F$ | Moles of ions in a feed |
| $n_D$ | Moles of ions in a draw solution |
| $Xi$ | Mole fraction of ions |
| $\gamma_{i,M}$ | Activity coefficients of ions in the mixture |
| $\gamma_{i,F}$ | Activity coefficients of ions in the feed |
| $\gamma_{i,D}$ | Activity coefficients of ions in the draw solution |
| $\gamma_s$ | Activity of solute |
| $v$ | Dissociation constant |
| $c$ | Molar concentration |
| $\Phi$ | Volumetric mixing ratio |
| $B$ | Mass fraction of water |
| $Mo$ | Molal concentrations |
| $\phi_m$ | Mass based mixing ratio |
| $v$ | Dissociation constant |
| $C$ | Molar concentration of the NaCl solution |
| $\gamma$ | Activity coefficient of ions |
| $\phi$ | Volumetric mixing ratio of the NaCl solution |
| $W$ | Power density |
| $\Delta P$ | Hydraulic pressure gradient |
| $W_{max}$ | Maximum power density |
| $D_w$ | Diffusion coefficient of water |

| | |
|---|---|
| $C_w$ | Concentration of water |
| $X$ | The axis perpendicular to the membrane surface |
| $\Delta\mu$ | Chemical potential difference between the feed and draw solution |
| $\Delta\mu_w$ | Transmembrane pressure difference at a constant temperature |
| $\alpha w$ | Chemical activity |
| $\bar{V}_w$ | Partial molar volume of water |
| $J_w$ | Water flux |
| $A$ | Water permeability coefficient |
| $C(x)$ | Solute concentration at area x |
| $D_{s.l}$ | Diffusion coefficient at the sublayer |
| $D$ | Diffusion coefficient |
| $\varepsilon$ | Porosity |
| $T$ | Tortuosity |
| $\Delta Cs$ | Solute concentration gradient |
| $C_s$ | Solute concentration |
| $D_s$ | Diffusivity of draw solute across the membrane |
| $\delta_m$ | Membrane thickness |
| $B$ | Solute permeability coefficient |
| $R$ | Salt rejection |
| $Re$ | Reynolds number |
| $Sc$ | Schmidt number |
| $L$ | Channel length |
| $J_s$ | Solute flux |
| $C_i$ | Solute concentration at the active layer interface |
| $\beta$ | Van't Hoff factor |
| $x$ | Distance from the interface between the support and the active layers |
| $C_{icp}$ | Solute concentration at this x area |
| $C_{F,m}$ | Feed solution concentration |
| $t_s$ | Thickness of the support layer |
| $k$ | Mass transfer resistance to salt within the support layer of the membrane |
| $k_L$ | Mass transfer coefficient |
| $k_D$ | Mass transfer coefficient on the draw side |
| $k_F$ | Mass transfer coefficient on the feed side |
| $\pi_{D,b}$ | Osmotic pressure of the draw solution |
| $\pi_{F,b}$ | Osmotic pressure of feed solution |
| $C_{F,b}$ | Salt concentration of the bulk feed solution |
| $C_{D,m}$ | Salt concentration of the bulk draw solution at the membrane surface |

| | |
|---|---|
| $K$ | Solute resistivity of the porous membrane support |
| $C_{D,b}$ | Draw solution concentration |
| $\delta_D$ | Thickness of the draw boundary layer |

## 1. Introduction

The world is currently experiencing rapid population growth, industrialization, and economic development, which lead to a higher demand for accessible energy [1, 2]. The global energy use is highly dependent on fossil fuels, which are not only renewable, but also a primary cause of greenhouse gas emissions and global warming. Among the fossil fuels from which our energy is typically sourced are petroleum, coal, and natural gas [3], and the amount of fossil fuel reserves is exponentially declining [4]. Moreover, the worldwide surface temperature has in fact faced an increase in the last century. This has led to an increase in coastal erosion, flooding frequency, vegetation and livestock mortality, food shortage, illness prevalence, and destruction of several terrestrial and marine ecosystems [5]. Currently, several technologies have been continuously in study to provide sustainable and efficient solutions for the energy crisis. Technologies for more efficient production, processing, and distribution of energy are currently in various stages of development and implementation. Furthermore, a shift in the population's lifestyle has started to be noticeable, as societies, people, and enterprises have become more mindful of how energy use plays a vital role in the total energy requirement and crisis.

Due to the world demand for environmentally sustainable renewable energy, interest in cost-efficient, clean, and sufficient alternative sources has increased. Currently, these non-conventional renewable energy sources include solar, tide, wave, geothermal, wind, and biomass [6-9]. While research on these alternative sources and technologies has been consistently done, widespread use of these renewable energy sources is impeded by uneven availability of the resources and high cost of installation and maintenance [10]. Should the use of renewable energy sources be widely developed and implemented, this will lead to benefits which include, but are not limited to, environmental and economic sustainability and environmental safety [11].

Another renewable and sustainable energy source is salt gradient power [12]. The mixture of two streams, freshwater and saltwater, produces this energy. The free energy is released as driven by the chemical potential difference between the two water streams [13]. According to previous studies, the potential power

which can be harnessed worldwide from the mixing of river water and saltwater will exceed 2 TW [14, 15]. Filtration and membrane technology have played a huge part in provision of fresh and clean water supply from a number of sources, such as surface runoff, aquifers, freshwater, brackish water, saltwater, and even wastewater and industrial effluents [16, 17]. Membrane-based technologies do not only have the ability to treat water and recover valuable materials, but also manage treatment with less number of unit operations and high viability for a larger scale application [18]. Membranes for such processes are characterized on the basis of the mechanical and chemical properties, as well as permeability and selectivity [19]. In recent, studies on membrane-based technologies are continuously evolving, with researchers coming up with better approaches on the processes and better membranes for more efficient separation and suitability in various applications. It is highly predicted that membrane technology can sustainably manage the earth's water resources, especially in areas of high aridity [20]. It is then remarkable to be able to find a membrane-based technology which can augment the world's requirements for both fresh water and energy altogether. A number of membrane-based technologies have surfaced to harness salinity gradient power, such as reverse electrodialysis (RED), capacitive mixing (CapMix), battery mixing (BattMix), and pressure retarded osmosis (PRO) [21, 22].

PRO is a process currently being developed to provide solutions for worldwide problems in finding alternative renewable energy sources [21, 23]. While also capable of desalination and wastewater treatment, PRO mainly generates osmotic power, or the energy generated by the mixture of salt concentration difference between two streams, commonly freshwater and saltwater [24]. Moreover, desalination of concentrated brine can also be performed using PRO. PRO utilizes a semi-permeable membrane which is positioned between these two streams, allowing fresh water to flow from the less concentrated stream towards the direction of the more concentrated one, in order to achieve concentration gradient equilibrium between the two streams. Electricity is then produced using hydro turbines, like how hydropower energy is produced. The similarity between osmotic energy and hydropower ends there, since a hydropower plant

utilizes river water and dam, whereas PRO utilizes, as earlier mentioned, osmotic pressure gradient between two streams of different salinities. In PRO, the hydro turbine depressurizes the permeate to obtain power. This energy-generating aspect of PRO is highly promising in harnessing renewable energy to significantly lessen our dependency on fossil fuels and the high carbon footprint associated with it.

Nevertheless, membrane fouling/scaling is a crucial problem when using wastewater feed or seawater. Fouling of membranes can be divided into organic, inorganic and biofouling which influence the efficiency of the desalination technology [25]. The use of wastewater concentrate containing various foulants and scalants causes fouling problem. The fouling becomes severe when the wastewater is against the porous membrane sublayer rather than the active layer of the thin film composite (TFC) PRO membrane [26]. It was realized that when using wastewater concentrate feed in the PRO process, calcium phosphate salt becomes the predominant fouling. To mitigate fouling/scaling tendency of the PRO membrane, a suitable pre-treatment method is necessary. Researchers have developed different mitigation strategies for PRO membrane to reduce fouling problem [27-29]. These strategies can minimize the operating cost relating to membrane cleaning and ensure long term performance of the PRO membrane.

This review aims to introduce the various phenomena associated with pressure retarded osmosis process, as well as the recent development in membranes and modules' engineering specifically for the PRO process. In this review, different advanced hybrid PRO processes, advanced configurations, and niche applications for the PRO system were also discussed. Several review articles on PRO have been published recently; however, this review aims to provide a comprehensive look at all the PRO membrane and development, as well as put the spotlight on the wide range of applications for PRO, whether as a stand-alone process or a process integrated in a hybrid system. In fact, this review article is the first one to report the niche applications of PRO, which include, but not limited to, pool PRO, fertilizer-driven PRO, PRO for oil recovery, and geothermal PRO. Furthermore, this review exhausts all membrane development efforts for

PRO, and, in the authors' best knowledge, this review is also the first to report on the development of free-standing PRO membranes.

## 2. Theoretical background

### 2.1 Salinity gradient energy

A stream with lower solute concentration, known as the feed solution (FS), is separated from the draw solution (DS), another stream with higher solute concentration, by a semi-permeable membrane, which is only permeable for the solvent and impermeable for the solute. Due to the difference in the solute concentration of the two streams, both the FS and DS have different chemical potentials, μ. The osmotic pressure $\Delta\pi$ between the FS and DS is due to the concentration difference between these two streams, and the solvent (water, in this case) flows from the low-concentrated FS to the high-concentrated DS until equilibrium is reached. The transport of water through the semi-permeable membrane is known to be osmosis [30-32]. During the osmotic phenomenon, the DS is effectively diluted by the FS and the feed is concentrated simultaneously, until the chemical potential of the two streams across the membrane approaches equilibrium state. The osmotic pressure ($\pi$) of a solution can be obtained from the amount of the solute particles (n, mol), the solvent volume ($V_w$, L), and temperature (T, K), as shown in:

$$\pi = \frac{n}{V_m} iRT \quad (1)$$

where R is the ideal gas constant (8.314 x $10^{-2}$ bar L $K^{-1}$ $mol^{-1}$) and i is the dimensionless Van't Hoff factor [33]. The osmotic pressure difference causes the free energy released during the spontaneous mixing of the FS and the DS [34, 35]. This free energy can be theoretically calculated from the basic thermodynamics [31], wherein the Gibbs free energy of mixing ($\Delta G_{mix}$) freshwater and salt water is given by:

$$\Delta G_{mix} = G_B - (G_F + G_S) \quad (2)$$

where, $G_B$, $G_F$, *and* $G_S$ are the Gibbs free energies (J $mol^{-1}$) of brackish water resulting from the mixing of freshwater and salt water, freshwater, and salt water, respectively. The amount of Gibbs free energy which can be harnessed is basically a factor of the salinity difference between the two solutions mixed. As mentioned earlier, the reversible spontaneous mixing of freshwater and saltwater results in the production

of work. The spontaneity of mixing is given by the Gibbs free energy, $\Delta G_{mix}$, which is a function of the enthalpy of mixing ($\Delta H_{mix}$) and entropy of mixing ($\Delta S_{mix}$):

$$\Delta G_{mix} = \Delta H_{mix} - T\Delta S_{mix} \quad (3)$$

For an ideal solution, $\Delta H_{mix} = 0$, thus $\Delta G_{mix}$ can simply be derived from temperature and $\Delta S_{mix}$, which is the total molar entropy of the freshwater, saltwater, and the resultant brackish water streams during the mixing process. The calculated Gibbs free energy of mixing is known to be the theoretical maximum energy which can be produced during the mixing process [36]. When the water flux transports from the saline feed stream to the concentrated draw stream at almost constant pressure, the PRO process converts the osmotic pressure into hydraulic pressure. This results in an increase of the permeate volume generating a high amount of Gibbs free energy of mixing ($\Delta G_{mix}$) [37]. The general equation of $\Delta G_{mix}$ of the two different salinity solutions in an ideal process can be expressed as [34]:

$$-d(\Delta G_{mix}) = -RT\, ln(a_s dn_s) = \pi_{ss}\bar{V}_s dn_s \quad (4)$$

in which, T and R denote the absolute temperature and the gas constant. $a_s$, $n_s$, $\pi_{ss}$, and $\bar{V}_s$ are the activity coefficient of the product solution, the number of moles of the product solution, the osmotic pressure of the salty solution, and the molar volume of the final solution.

It is assumed that the extractable energy from PRO is equal to molar Gibbs free energy of mixing. The formula of the extractable energy can be written as:

$$\frac{-\Delta G_{mix}}{RT} = \sum_i X_{i,M}\, ln\left(\gamma_{i,M} X_{i,M}\right) - \frac{n_F}{n_M}\sum_i X_{i,F}\, ln\left(\gamma_{i,F} X_{i,F}\right) - \frac{n_D}{n_M}\sum_i X_{i,D}\, ln\left(\gamma_{i,D} X_{i,D}\right) \quad (5)$$

Herein, $n_M$, $n_F$ and $n_D$ describe the moles of ions in a mixture, FS, and DS, respectively. *Xi, M, F,* and *D* are the mole fraction of ions in the mixture, FS and DS while $\gamma_{i,M}, \gamma_{i,F}$, and $\gamma_{i,D}$ are the activity coefficients of ions. When saline solutions with different mixing ratio are used in the PRO process, this equation can

be modified as follows:

$$\frac{-\Delta G_{mix,V_A}}{vRT} \approx \frac{C_{s,M}}{\varphi}\ ln\left(\gamma_{s,M}C_{s,M}\right) - C_{s,A}\ ln\ \left(\gamma_{s,A}C_{s,A}\right) - \frac{1-\emptyset}{\emptyset}.C_{s,B}\ ln\left(\gamma_{s,B}C_{s,B}\right) \qquad (6)$$

In this equation, the activity of solute $(\gamma_s)$ is equal to 1. $v$ is the dissociation constant which is equivalent to 2 for NaCl solution. *c* and $\phi$ describe the molar concentration and the volumetric mixing ratio. "M", "A", "S" and "B" are the mixture fluid, the fresh water feed, the DS, and the mass fraction of water, respectively.

It should be noted that this equation is not valid for highly concentrated salt solutions. Thus, it can be rephrased to calculate the mixing energy for highly concentrated salt solutions as follows:

$$\frac{-\Delta G_{mix,M_A}}{RT} = \frac{Mo_{w,M}}{\varphi}\ ln\left(\gamma_{w,M}X_{w,M}\right) + \frac{v.mo_{s,M}}{\varphi}\ C_{s,A}ln\left(\gamma_{s,M}X_{s,M}\right) -$$

$$mo_{w,A}\ ln\left(\gamma_{w,A}X_{w,A}\right)\ -\ v.mo_{s,A}\ ln\left(\gamma_{s,A}X_{s,A}\right) - \frac{mo_{w,B}.(1-\varphi)}{\varphi m}\ ln\left(\gamma_{w,B}X_{w,B}\right) - \qquad (7)$$

$$\frac{v.mo_{s,B}.(1-\varphi_m)}{\varphi m}\ ln\left(\gamma_{s,B}X_{s,B}\right)$$

where $M_o$ and $\phi_m$ referred to the molal concentrations and the mass-based mixing ratio. *s, v,* and *c* denote the salt, the dissociation constant, and the molar concentration of the NaCl solution, respectively. The activity coefficient of ions, and the volumetric mixing ratio of the NaCl solution are represented as $\gamma$ and $\phi$, respectively. By using this equation, it is possible to calculate the amount of energy extracted from mixing two different saline solutions in an isothermal and isobaric process. This equation indicates that increasing the concentration of the DS results in higher energy generation. The increase in volume of the pressurized DS effectively increases the pressure. The resultant diluted DS during the PRO process is then directed toward two different streams: (1) the hydro-turbine, for energy production, and (2) the pressure exchanger, for energy recovery [38, 39].

2.2. Water permeability

According to solution-diffusion model, the water permeate through the membrane can be determined using

the following formula [34]:

$$J_w = -D_w \frac{dc_w}{dx} \quad (8)$$

where $D_w$ and $C_w$ are the diffusion coefficient of water and the concentration. $X$ is the axis perpendicular to the membrane surface. When including the chemical potential difference $(\Delta\mu)$ between the feed and draw streams, the gas constant ($R$), and the absolute temperature ($T$), Eq. (8) becomes:

$$J_w = \frac{D_w c_w}{RT}\frac{d\mu_w}{dx} \approx \frac{D_w c_w}{RT}\frac{\Delta\mu_w}{\Delta x} \quad (9)$$

where $\Delta\mu_w$ represents the transmembrane pressure difference at a constant temperature. The transmembrane difference can be computed considering the chemical activity ($\alpha_w$) and the partial molar volume of water ($\bar{V}_w$). The equation can be expressed as:

$$\Delta\mu_w = RT\ ln\ \Delta\alpha_w + \bar{V}_w \Delta P \quad (10)$$

The water activity of water can also be used to measure the osmotic pressure as follows:

$$\Delta\pi = -\frac{RT}{\bar{V}_w} ln\ \alpha_w \quad (11)$$

This model can be rearranged when replacing $RT\ ln\ \Delta\alpha_w$ with $\bar{V}_w\Delta\pi$ as follows:

$$\Delta\mu_w = -\bar{V}_w\Delta\pi + \bar{V}_w\Delta P = \bar{V}_w(\Delta P - \Delta\pi) \quad (12)$$

When putting together Eq. 10 and 12, the water flux equation can be calculated using Eq.(14):

$$J_w = \frac{D_w C_w \bar{V}_w}{RT\Delta x}(\Delta P - \Delta\pi) = A(\Delta P - \Delta\pi) \quad (13)$$

In general, there is a strong correlation among water flux ($J_w$), the osmotic pressure difference ($\Delta\pi$), and the applied pressure difference ($\Delta P$). Besides, the expression $\frac{D_w C_w \bar{V}_w}{RT\Delta x}$ equals to the water permeability coefficient ($A$) [40]. Therefore, the water flux within a semi-permeable membrane when assuming an ideal mixing of salt solutions can be written as [41, 42]:

$$J_w = A\ (\pi_D - \pi_F) \quad (14)$$

$J_w$ and $A$ are the water flux and the water permeability coefficient through the membrane, respectively. $\pi_D$

and $\pi_F$ denote the bulk osmotic pressures of the draw and feed streams, respectively. In contrast, this equation is not reliable to predict the mass transfer on both the feed and draw streams and within the support layer of the selected membrane [41]. It is because the reverse solute flux and concentration polarizations affect the transport of water flux through the membrane and the efficiency of power production. Pure water permeability constant $A$ can be calculated as:

$$A = \frac{\Delta V}{A_m \Delta t \Delta P} \tag{15}$$

where $\Delta V$, $A_m$, and $\Delta t$ are permeate volume, effective membrane area, and sampling time, respectively [43].

2.3. Power density

In PRO, power generated per unit membrane area (W $m^{-2}$) is known as the power density, $W$, given by this equation:

$$W = J_w \Delta P = A(\Delta\pi - \Delta P)\Delta P \tag{16}$$

where, W is the product of the water flux and the hydraulic pressure applied across the membrane [44]. With respect to ΔP, the maximum power density can be obtained when ΔP is equal to half of the osmotic pressure difference across the membrane, as shown in Figure 1. The equation for the maximum power density can be expressed as:

$$W_{max} = A\frac{\Delta\pi^2}{4} \tag{17}$$

The $W_{max}$ during a PRO operation is directly proportional to the pure water permeability, $A$, and the square of the osmotic pressure difference across the membrane, thus the maximum power generation can be obtained when PRO is operated at a pressure close to $\frac{\Delta\pi}{2}$, as shown in Figure 1.

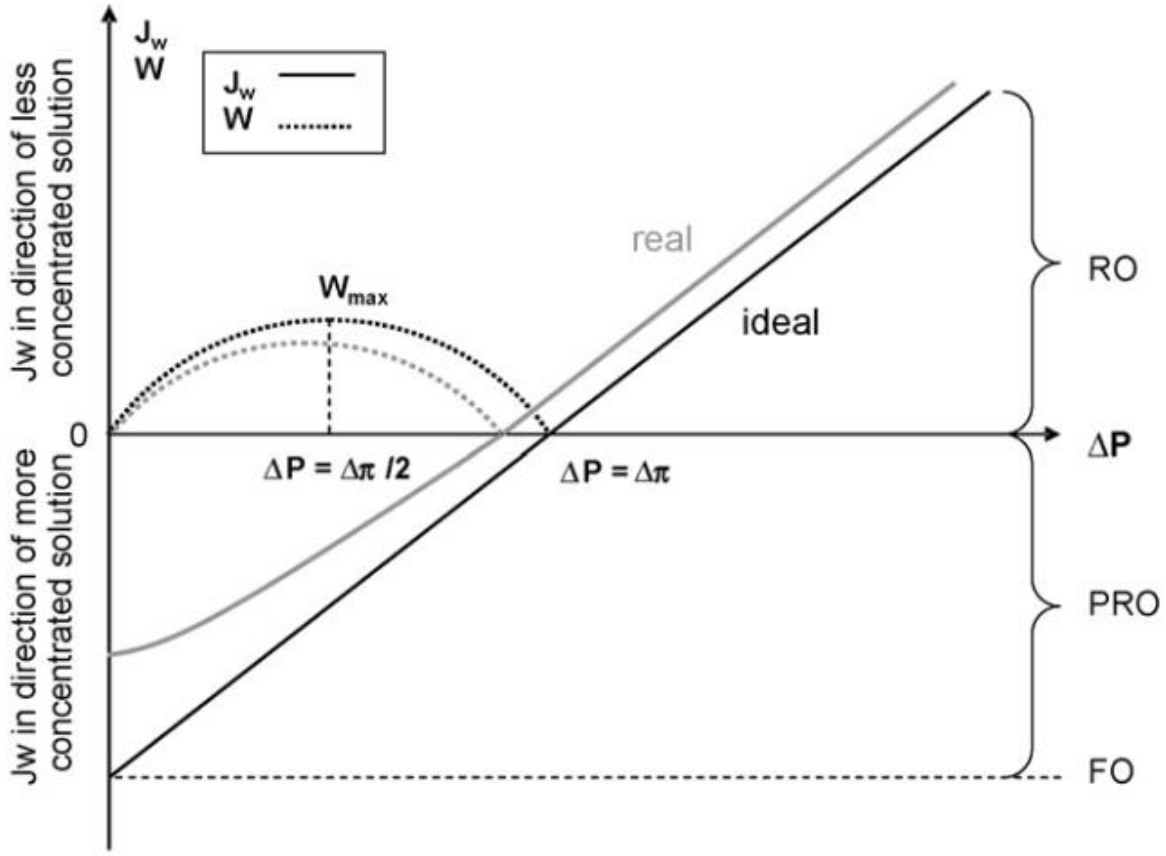


Figure 1. The ideal water flux ($J_w$) and power density ($W$) during PRO operation as a function of applied hydraulic pressure ($\Delta P$). The conditions surrounding FO, PRO, and RO operation are also shown. [45].

However, it should be noted that the maximum power density in real PRO system is quantified according to the water flux, reverse solute flux, concentration polarizations, the operating parameters and the selected membrane [41]. The performance of the PRO membranes can be accurately evaluated in terms of the water flux and reverse solute flux.

2.4. Solute permeability

Due to the non-ideality of the semi-permeable membrane, it is possible that solute can permeate from the DS toward the FS, in a phenomenon known as reverse salt flux (RSF). The RSF leads to a decrease in the effective osmotic pressure difference across the membrane. This salinity displacement, or the flow of the DS within the support layer, results from of the convection and diffusion transfer of the solute in the

support layer [34]. The reverse solute flux can be determined using Fick's law as follows:

$$J_s = D_{s.l}\frac{dC(x)}{dx} - J_w C(x) \tag{18}$$

where $C(x)$ describes the solute concentration at area $x$ while $D_{s.l}$ refers to the diffusion coefficient at the sublayer. The later can be measured considering the diffusion coefficient ($D$), the porosity ($\varepsilon$) and the tortuosity ($\tau$) of the support layer. The equation can be derived as:

$$D_{s.l} = \frac{\varepsilon D}{\tau} \tag{19}$$

By combining the solute concentration gradient ($\Delta C_s$) within the membrane, the RSF is given by:

$$J_s = -D_s\frac{dC_s}{dx} \simeq D_s\frac{\Delta C_s}{\delta_m} \tag{20}$$

in which $C_s$, $D_s$, and $\delta_m$ are the concentration, diffusivity of draw solute across the membrane, and the membrane thickness, respectively. The workable RSF equation is written as:

$$J_s = B\Delta C_m \tag{21}$$

where $B$ is defined as the solute permeability coefficient, which can be determined from membrane salt rejection ($R$), according to the following equations [43]:

$$R = \left(1 - \frac{C_d}{C_f}\right) \tag{22}$$

$$B = J_w\left(\frac{1-R}{R}\right)e^{-\frac{J_w}{k_L}} \tag{23}$$

where $C_d$, $C_f$, and $k_L$ are the DS solute concentration, FS solute concentration, and mass transfer coefficient, respectively [46]. $k_L$ can be determined from the Sherwood number ($Sh$), solute diffusion coefficient ($D_s$), and the cross-flow cell hydraulic diameter ($d_h$), which are based on the hydrodynamic conditions during an engineered osmosis process, and these parameters can be calculated from the following equations:

$$k_L = \frac{Sh \cdot D_s}{d_h} \tag{24}$$

$$Sh = 1.85\left(Re \cdot Sc\frac{d_h}{L}\right)^{0.33} \text{ if } Re < 2000 \tag{25}$$

$$Sh = 0.04 \cdot Re^{0.75} \cdot Sc^{0.33} \text{ if } Re > 2000 \tag{26}$$

where $Re$, $Sc$, and $L$ are Reynolds number, Schmidt number, and channel length, respectively [47].

Upon determination of *B,* the value of RSF, $J_s$, can be determined by this equation [48]:

$$J_s = B\,(C_d - C_i) \tag{27}$$

where $J_s$ *and* $C_i$ are the solute flux and the solute concentration at the active layer interface, respectively.

In addition, the specific salt flux is another technical obstacle affecting the water permeation across the membrane. It is defined as the ratio of the salt flux to the water flux $J_s/J_w$ [37]. It can be controlled by the hydraulic pressure gradient ($\Delta P$) on the membrane, the water permeation ($J_w$), the water permeability coefficient ($A$), and the solute permeability coefficient ($B$). The equation of the specific salt flux including the van't Hoff factor ($\beta$) is provided by:

$$\frac{J_s}{J_w} = \frac{B}{A\beta RT}\left(1 + \frac{A\Delta P}{J_w}\right) \tag{28}$$

It is worth noting that the RSF expression can be combined with concentration polarization expressions to derive the final model of the water flux.

2.5. Concentration polarization

During PRO operation, an amount of salt is able to permeate through the semi-permeable membrane, significantly affecting the concentration gradient across the membrane. This then leads to the extraction of lower power density compared to the theoretical power density. The change in concentration gradient across the membrane causes reduction of water flux across the membrane; however, another phenomenon responsible for water flux decline during osmotic operation is concentration polarization.

Concentration polarization (CP) is a naturally occurring phenomenon due to the accumulation of solute particles near the membrane interface or within the support layer. CP especially occurs during processes utilizing asymmetric composite membranes, where a thin dense polyamide selective layer is on top of a porous membrane support. CP is classified into external and internal concentration polarization. Solute particles tend to accumulate on the dense layer side (external CP, or ECP), or internally, on the interface

between the membrane support and selective layer (internal CP, or ICP). Due to the occurrence of CP, the actual osmotic pressure difference across the membrane is less than the osmotic pressure difference of the bulk fresh and draw streams, and the consequence of which is water flux decrease [49]. It is true that CP is not only influenced by the membrane design and transport properties, it is also influenced by the system specifications and design, hydrodynamics, and operating parameters. Figure 2 shows the concentration profile in a PRO membrane during PRO orientation due to CP.

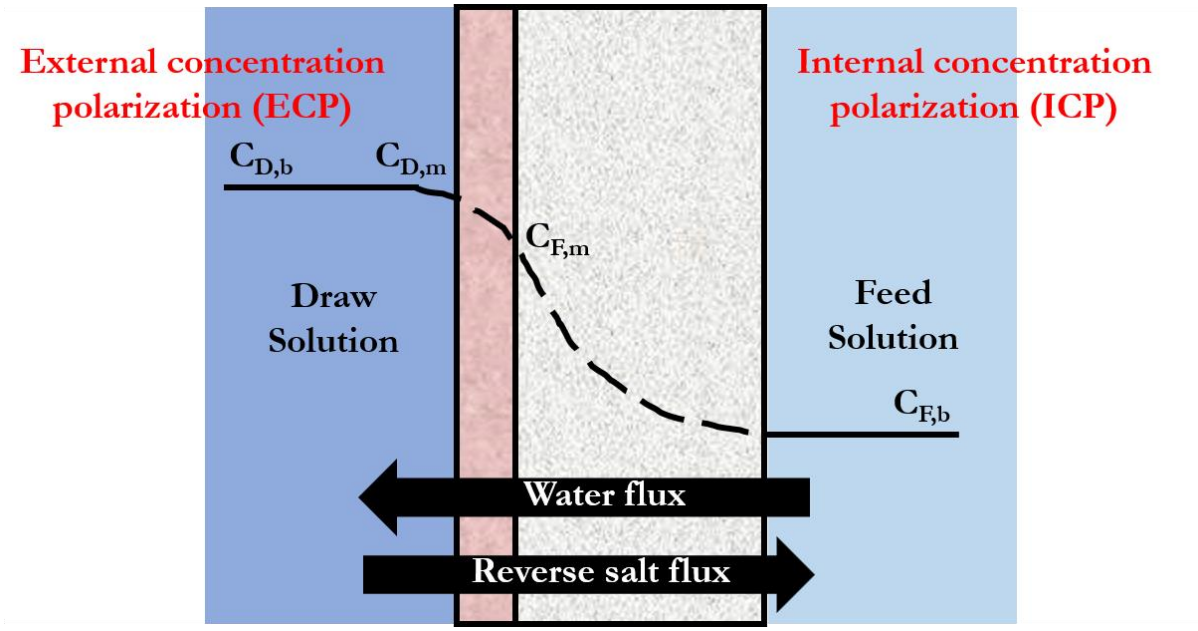


Figure 2. The concentration profile of the membrane during PRO operation as influenced by ECP and ICP. $C_{D,b}$, $C_{D,m}$, $C_{F,b}$, and $C_{F,m}$ are the concentration of the bulk draw solution, concentration of the draw solution at the membrane active layer interface, concentration of the feed solution at the support and active layer interface, and concentration of the bulk feed solution, respectively.

One main factor affecting the occurrence of CP in osmotic processes is the membrane orientation. Asymmetric membranes typically have a porous support and a solute-rejecting active layer. For osmosis-driven processes, the active layer can have either one of the following orientations: (1) active layer facing the FS (AL-FS), or (2) active layer facing the DS (AL-DS). In the case of PRO, operation is conventionally performed with AL-DS membrane orientation, meanwhile other osmotic-driven processes, such as forward osmosis (FO) and pressure assisted

osmosis (PAO) are typically operated at AL-FS membrane orientation.

*2.5.1. Internal concentration polarization*

Generally, ICP is caused by the inability of the solute particles to pass through the membrane active layer; therefore, ICP is heavily influenced by solute molecular size and diffusivity. ICP specifically occurs within the porous membrane support layer as the solutes of the DS accumulates at the interface of the support and the active layers, due to the inability of the solute particles to penetrate and pass through the dense active layer [50]. An immobile area is formed inside the membrane support, decreasing the osmotic driving force [51, 52].

By considering the effect of ICP, the RSF (Eq. (27)) including the boundary conditions can be rephrased as [34]:

$$C_{icp} = \left(C_{F,m} + \frac{J_s}{J_w}\right)\exp(J_w k) - \frac{J_s}{J_w} \tag{29}$$

where

$$\begin{cases} C(x=0) = C_{F,m} \\ C(x=t_s) = C_{icp} \end{cases} \tag{30}$$

in which, $x$ is the distance from the interface between the support and the active layers. $C_{icp}$ and $C_{F,m}$ are the solute concentration at this area, and the FS concentration. $t_s$ referred to the thickness of the support layer. The equation of the effective osmotic pressure gradient across the selective layer can be expressed as:

$$\Delta\pi_{eff} = \pi_c - \pi_d \exp(J_w k) \tag{31}$$

where $k$ describes the mass transfer resistance to salt within the support layer of the membrane, and $\exp(J_w k)$ represents the internal concentration polarization expression. By combining the ICP expression and the mass transfer coefficients on the draw side ($k_D$) and on the feed side ($k_F$) into the water flux Eq.(15), this equation can be rewritten as:

$$J_w = A\left[\pi_{D,b}\exp\left(\frac{-J_w}{k_D}\right) - \pi_{F,b}\exp\left(\frac{J_w}{k_F}\right)\right] \tag{32}$$

where $\pi_{D,b}$ and $\pi_{F,b}$ are the osmotic pressure of the DS and FS.

This equation can be modified when applying the hydraulic pressure on the feed side. This is due to low osmotic pressure gradient and sever ICP effects. Thus, Eq.(15) can be rewritten as:

$$J_w = A\left(\Delta P + \pi_{D,b}\exp\left(-\frac{J_w}{k}\right)\right) \tag{33}$$

where $\pi_{D,b}$ and $k$ denote the bulk osmotic pressure of the DS and the mass transfer coefficient in the boundary layer across the active layer.

The effect of ICP on the PRO performance is given by this equation [44]:

$$J_w = A\left[\pi_{D,m}\frac{1-\frac{C_{F,b}}{C_{D,m}}e^{J_wK}}{1+\frac{B}{J_w}(e^{J_wK}-1)}\right] - \Delta P \tag{34}$$

where $C_{F,b}$ and $C_{D,m}$ are the salt concentrations of the bulk FS and DS at the membrane surface, respectively. This model suggests that ICP generally occurs due to the presence of the membrane substrate layer. $K$ is the solute resistivity of the porous membrane support for the diffusion of solute particles, and can be determined using the following equation [53]:

$$K = \frac{t\tau}{D_s\varepsilon} = \frac{S}{D_s} \tag{35}$$

where $t$, $\tau$, $D_s$, $\varepsilon$, and $S$ are the membrane support porosity, membrane support thickness, membrane support tortuosity, diffusion coefficient of the solute in the DS, membrane support porosity, and structural parameter, respectively. $S$ is an important transport parameter in osmotic processes, as it provides a singular parameter describing the membrane porosity, thickness, and tortuosity, which could all influence the membrane permeability. By incorporating the solute resistivity (K), the concentration of the FS ($C_{F,b}$), the concentration of the DS ($C_{D,b}$), and ICP expression, the water flux equation can be rewritten as [34]:

$$J_w = A\left[\pi_{D,b}\frac{1-\frac{C_{F,b}}{C_{D,b}}\exp(J_wK)}{1+\frac{B}{J_w}\left[\exp(J_wK)-1\right]} - \Delta P\right] \tag{36}$$

It can therefore be said that these properties of the porous membrane support layer affect the occurrence

of ICP during PRO operation, and, consequently, affect the water flux.

*2.5.2 External concentration polarization*

ECP inhibits water flow due to the change in osmotic pressure at the membrane active layer surface. ECP can either be concentrative or dilutive, depending on the position of the active layer surface. If the active layer faces the feed side, the solute is concentrated at the membrane surface, resulting in concentrative ECP. On the other hand, dilutive ECP occurs when the solute is diluted around the membrane active layer facing the DS side.

The dilutive ECP expression can be expressed based on the boundary conditions. The boundary conditions involve the solute concentration at the interface of the selective layer ($C_{D,m}$), the draw concentration ($C_{D,b}$), the distance between the interface of the selective and support layers (x) and the thickness of the draw boundary layer ($\delta_D$). It can be derived as follows [34]:

$$C_{D,m} = \left(C_{D,b} + \frac{J_s}{J_w}\right) exp\left(-\frac{J_w}{k_D}\right) - \frac{J_s}{J_w} \tag{37}$$

where

$$C(x = 0) = C_{D,m}$$
$$C(x = \delta_D) = C_{D,b}$$

The concentrative ECP can be determined using Eq. (37):

$$C_{F,m} = \left(C_{F,b} + \frac{J_s}{J_w}\right) exp\left(-\frac{J_w}{k_F}\right) - \frac{J_s}{J_w} \tag{38}$$

where

$$C(x = 0) = C_{F,b}$$
$$C(x = \delta_F) = C_{F,m}$$

By considering the membrane intrinsic transport characteristics, the water flux equation can be modified as:

$$J_w = \left(\frac{1}{K}\right)\left[ln\ \frac{B + A\pi_{D,b}\ exp\left(-\frac{J_w}{k_L}\right) \times (R + (1-R)\exp\left(\frac{J_w}{k_L}\right)) - J_w}{B + A\pi_{F,b}\frac{\exp\left(\frac{J_w}{k_L}\right)}{\left(R + (1-R)\exp\left(\frac{J_w}{k_L}\right)\right)}}\right] \quad (39)$$

By incorporating the ICP, dilutive ECP, and the reverse solute diffusion, the water flux equation can be rewritten as:

$$C_{D,m} - C_{icp} = \left[\frac{C_{D,b}\ exp\left(-\frac{J_w}{k_L}\right) - C_{F,b}\ exp\left(\frac{J_w S}{D}\right)}{1 + \frac{B}{J_w}\left\{exp\left(\frac{J_w S}{D}\right) - exp\left(-\frac{J_w}{k_L}\right)\right\}}\right] \quad (40)$$

When incorporating Van't Hoff expression, Eq. (8) and (40), the final water flux equation becomes:

$$J_w = A\left[\frac{\pi_{D,b}\ exp\left(-\frac{J_w}{k_L}\right) - \pi_{F,b}\ exp(J_w K)}{1 + \frac{B}{J_w}\left\{exp(J_w K) - exp\left(-\frac{J_w}{k_L}\right)\right\}} - \Delta P\right] \quad (41)$$

Similarly, the final RSF can be rephrased as:

$$J_s = A\left[\frac{C_{D,b}\ exp\left(-\frac{J_w}{k_L}\right) - C_{F,b} exp(J_w K)}{1 + \frac{B}{J_w}\left\{exp(J_w K) - exp\left(-\frac{J_w}{k_L}\right)\right\}}\right] \quad (42)$$

Eventually, the water flux and reverse solute flux across the PRO membrane can be influenced significantly by the mass transfer characteristics of the membrane. The physicochemical properties of the selected membrane are other crucial elements that deteriorate both the water flux and the RSF. Not only they could acerbate the reverse solute flux and the ICP, they may also critically lower the osmotic driving force for power extraction [54]. Consequently, the development of high-performance PRO membranes with excellent water permeation and minimum reverse solute flux has increasingly attained attention in PRO research.

## 3. Fouling, scaling, and mitigation

One of the limitations of PRO is the occurrence of membrane fouling, which can be influenced by the

membrane orientation and application of hydraulic pressure during PRO operation. Typical feed streams for PRO contain huge amounts of colloidal particles, organic, inorganic, and biological matter that could induce fouling and affect membrane performance, *i.e.*, flux and power density reduction. Upon occurrence of fouling, there is a decrease in the membrane performance, which, in turn, limits the power generation and increases power consumption. Fouling can be caused by a number of fouling substances, or foulants, which can be classified into any of the following: inorganic, organic, colloidal, and biological. In PRO process, fouling mainly occurs in any one of these fouling mechanisms: (1) pore plugging, (2) pore narrowing, and (3) film or cake formation. Pore plugging occurs when larger foulant particles plug the membrane pores. In the case of smaller or finer foulant particles, these can absorbed into the membrane porous structure and accumulate inside the pores, effectively narrowing the pore size. Finally, film or cake formation occurs when the foulants are not absorbed into the pore, but accumulate on the membrane surface instead, effectively blocking the pore.

### 3.1. Fouling studies for PRO

Among the earliest PRO fouling studies was conducted by Yip et al., who investigated the influence of natural organic matter (NOM) [55] on membrane performance. It was found out that NOM, which is highly present in river water, could cause severe water flux decline to over 46%, following the adsorption of the foulants at the interface between the active layer and membrane substrate, resulting in higher transport resistance [55]. Thelin et al. also studied the effect of NOM, wherein the effect of NOM concentration and ionic strength in the feed stream was investigated [56]. The researchers found that the PRO membrane fouling propensity was independent of the NOM concentration, and instead was influenced by the increased ionic strength brought about by RSF and ICP.

Fouling due to organic substances, specifically, alginate, was found to be a major issue during PRO operation [57]. It was also found out in this study that alginate fouling was more severe when the DS contained large amounts of divalent cations, like $Ca^{2+}$ and $Mg^{2+}$. Interactions of inorganic species with organic foulants

enhanced organic fouling, especially at higher DS concentrations. Similarly, gypsum, or calcium sulfate dihydrate, was another foulant investigated and found to affect PRO operation performance [58]. Gypsum, formed from the interaction of calcium and sulfate present both in the feed and draw streams, was found to clog the pores of the membrane substrate and cause severe ICP.

Colloidal fouling, specifically, silica, was studied by Kim et al. [59]. The researchers found that colloidal fouling due to silica occurs through a cake layer buildup at the surface of the membrane. Furthermore, salt diffusion increased fouling occurrence due to the interaction of the salt with the cake layer, effectively reducing the osmotic driving force.

Mixed gypsum scaling and sodium alginate fouling was examined in a study, which concluded that in combined fouling studies, the membranes are initially conditioned or fouled more easily by a single foulant [60]. After the conditioning, the membrane surface chemistry changes, which accelerates the fouling occurrence of the other foulants. The presence of both gypsum and alginate during PRO operation allows the initial occurrence of alginate fouling, due to the lower gypsum scaling propensity due to reverse diffusion of $Na^+$; thus, alginate fouling conditions the membrane first, followed by the formation of gypsum scaling.

Combined fouling was investigated using real wastewater concentrate FS, using which, the main types of fouling include organic (humics and alginate) and inorganic (calcium phosphate and gypsum) fouling [61]. Similar to the study which used model foulants, the scaling caused by inorganic foulants contributed mainly to the decline in membrane performance. RO retentate was also used as feed stream in an earlier study, and it was found that calcium phosphate scaling and silica fouling were the biggest fouling problems, affecting the innermost layer and the outmost surface of hollow fiber membranes, respectively [62].

Biofouling propensity was investigated in another study, and it was found that biological population in the wastewater, when used as feed, could cause severe fouling both on the membrane substrate and feed spacer, and eventually cause severe flux decline [63].

3.2. Pre-treatment processes and fouling mitigation

Kim and Elimelech [38] were among the first ones to propose PRO configurations which include pretreatment of the feed stream to prevent the occurrence of membrane fouling, especially when municipal wastewater effluent would be used as feed instead of river water.

Abbasi-Garravand et al. proposed the use of a multimedia sand filter and ultrafiltration (UF) as pretreatment to eliminate total organic carbon (TOC), turbidity, and hardness of the FS prior to PRO operation [64]. Using the multimedia sand filter, 68.6% turbidity and 1.5% TOC were removed, while 100% turbidity and 41% TOC were removed using UF.

UF, nanofiltration (NF), and low-pressure reverse osmosis (LP-RO) were conducted in another study as pretreatment procedures of wastewater retentate, prior to use as feed stream in another study [65]. Among the three processes, while LP-RO was found to be able to most effectively mitigate fouling, NF was found to be the most effective in rejection of species such as calcium and phosphate ions which could form hydroxyapatite, a well-known scalant during PRO. Low-pressure NF was also performed by Chen et al., and they found that low-pressure NF could remove multivalent ions and NOM, which are both persistent foulants during PRO; however, silica fouling was not effectively prevented using this process [66].

Coagulation was performed as a pretreatment in a recent study [67]. Two coagulants, acidic $AlCl_3$ and alkaline $NaAlO_3$ were used to coagulate with phosphate to eliminate this particular species from the concentrated wastewater and prevent the formation of $Ca_3(PO_4)_2$. While both coagulants were effective in $PO_4^{3+}$, $AlCl_3$ was less effective in removal of silica, which leads to lower water flux recovery after hydraulic

backwashing.

Fouling caused by the use of real concentrated wastewater as FS for PRO was mitigated in a study which employed different pretreatments to remove foulants from the feed [62]. Both pH adjustment by adding HCl and removal of anti-scalant via chelation with ethylenediaminetetraacetic acid (EDTA) were successful in mitigating fouling, even after backwashing. Another study demonstrated similar findings when anti-scalant pretreatment and pH adjustment were found to be both effective for fouling control [68].

Kim et al. [69] investigated the possibility of PRO operation with the membrane active layer facing the feed stream (AL-FS), instead of the conventional membrane AL-DS membrane orientation, or the active layer facing the draw stream. They were able to demonstrate lower RSF during AL-FS operation, reduced pretreatment cost, and better fouling control due to the high shear flux caused by the water permeation from the FS toward the DS. While promising, this research was not followed up due to intrinsically lower membrane performance at AL-FS mode and issues with membrane deformation due to hydraulic pressure.

For continuous PRO operation, physical backwashing proves to be highly effective in removing fouling species from the porous support layer, leading to high recovery of membrane performance [55]. In another study, air bubbling was also found to be even more effective in removal of foulants on the membrane surface [62]. Various membrane cleaning agents were employed and compared for membrane cleaning and performance recovery ability. Among DI water, alkaline solution, acidic solution, and chelating solution, the chelating agent EDTA was found to be the most effective in recovering the performance of the membrane used for PRO with wastewater effluent as feed [70].

Chemical-in-place was introduced as a cleaning strategy for a laboratory-scale SWRO-PRO pilot study [71]. This chemical-free cleaning strategy uses continuous circulation of tap water directed to both the outer

surface and inner surface of hollow fiber membranes. This particular strategy resulted to excellent water permeability recovery, without affecting its operational duration, especially during intermittent chemical-in-place cleaning.

Larger scale demonstrations using larger membrane modules may perform chemical-involving maintenance cleaning for the membranes by flushing the fouled membranes with low-concentration acidic or alkaline solution, with tap water circulated concurrently. This treatment, however, is longer than chemical-in-place, due to several cycles of recirculation and soaking [71].

### 3.3. Anti-fouling PRO membranes

Several PRO membrane development studies were conducted focusing on mitigation of the fouling propensity during PRO operation.

Alginate fouling, influenced by $Na^{2+}$, was reduced by using annealed PBI/POSS/PAN hollow fiber membranes [72]. The membrane selectivity was enhanced, since reverse diffusion of NaCl results in increased alginate fouling. Since then, anti-fouling membrane development studies have mainly focused on chemical modification or incorporation of nano-sized materials with intrinsic hydrophilicity and functionality, whose interaction with foulants could control fouling. Chemical modifications of membranes used various agents, among which are polyvinyl alcohol and polydopamine [73], polyelectrolytes [74], zwitterions [75-77], aminosilane [78], hyperbranched polyglycerol [79, 80], and hyperbranched poly(ionic liquid) [81]. Among the nano-sized materials in literature are carbon quantum dots [82], carbon nanotubes [83], titanium dioxide [84], graphene oxide, and halloysite nanotubes [85]. Silver nanoparticles, known for their biocidal properties, have been also incorporated in membranes specifically designed for biofouling mitigation [86]. There are a number of studies which used different membrane preparation technique, such as double polyamide active layers for both ICP and fouling mitigation [87]. More information on PRO membrane development will be discussed in the succeeding chapter.

## 4. Membrane development for pressure retarded osmosis

An immensely vital aspect of the PRO process is the use and development of suitable and highly efficient membranes, such that it was deemed practically and economically not feasible to proceed with PRO commercialization and further development without suitable membranes [88]. Due to the similarities of PRO with reverse osmosis (RO) (i.e., application of hydraulic pressure and membrane orientation), asymmetric RO membranes were used during the initial studies on PRO [33, 89-91]. Immensely low performance was obtained from the earliest studies due to the thick supports of those membranes, which caused ICP to occur and led to low water flux and power density.

Initially, cellulose-based membranes were used for the initial PRO studies, due to its commercial availability, as well as hydrophilicity and satisfactory tensile strength. A flat-sheet cellulose acetate membrane was prepared and was developed specifically for desalination [53, 92]. These integrated skinned cellulose-based membranes were either cellulose acetate (CA) or cellulose triacetate (CTA). Hydration Technologies Inc. (HTI) developed a cellulose-based membrane for FO and PRO applications, which was utilized in the earlier PRO simulations [38, 45]. The HTI membrane became the standard commercially available membrane, until targeted osmotic energy requirements during large-scale PRO implementation could not be achieved by the HTI membrane, and therefore requiring the use of a different type of membranes [31, 93].

Several studies on membrane development have been performed, and a significant number has been used for industrial applications. Since then, advanced materials and sophisticated methods have paved the way to continuous improvement of membrane properties and performance. A vast improvement in the membranes' chemical and thermal stability, as well as transport properties, can be observed on the membranes currently in development, compared to the very first membrane for an osmotic process. Based on the various mathematical simulation of PRO, PRO membrane design has specifically focused on the following membrane characteristics: (1) hydrophilicity, for enhanced water flux and fouling mitigation; (2)

selectivity of the thin, dense active layer for satisfactory solute rejection; and (3) high tensile strength to withstand the application of hydraulic pressure. Development of suitable PRO membranes made it possible to achieve higher power density values, which further shows the feasibility of PRO for wider-scale applications.

### 4.1. Flat sheet TFC PRO membranes

Thin film composite (TFC) membranes, known to be asymmetric, are consisted of two layers: (1) a microporous membrane substrate, and (2) a dense, selective thin film, typically polyamide formed in situ on the membrane substrate surface via interfacial polymerization (IP) [94]. The membrane supports are conventionally prepared either via nonsolvent-induced phase separation (NIPS) or electrospinning of polymeric substances. During NIPS, the polymer solution was made in contact with a nonsolvent (conventionally, water), resulting to coagulation and phase separation of the polymer. The most common PA active layer for PRO TFC membranes is formed from the following monomers: *m*-phenylenediamine (MPD) and trimesoyl chloride (TMC) [95, 96]. Figure 3 shows the typical morphology of a flat sheet TFC PRO membrane, whose substrate is prepared via NIPS. Flat sheet membranes gained popularity due to ease in preparation of the membranes, as well as the application for plate-and-frame and spiral wound modules.

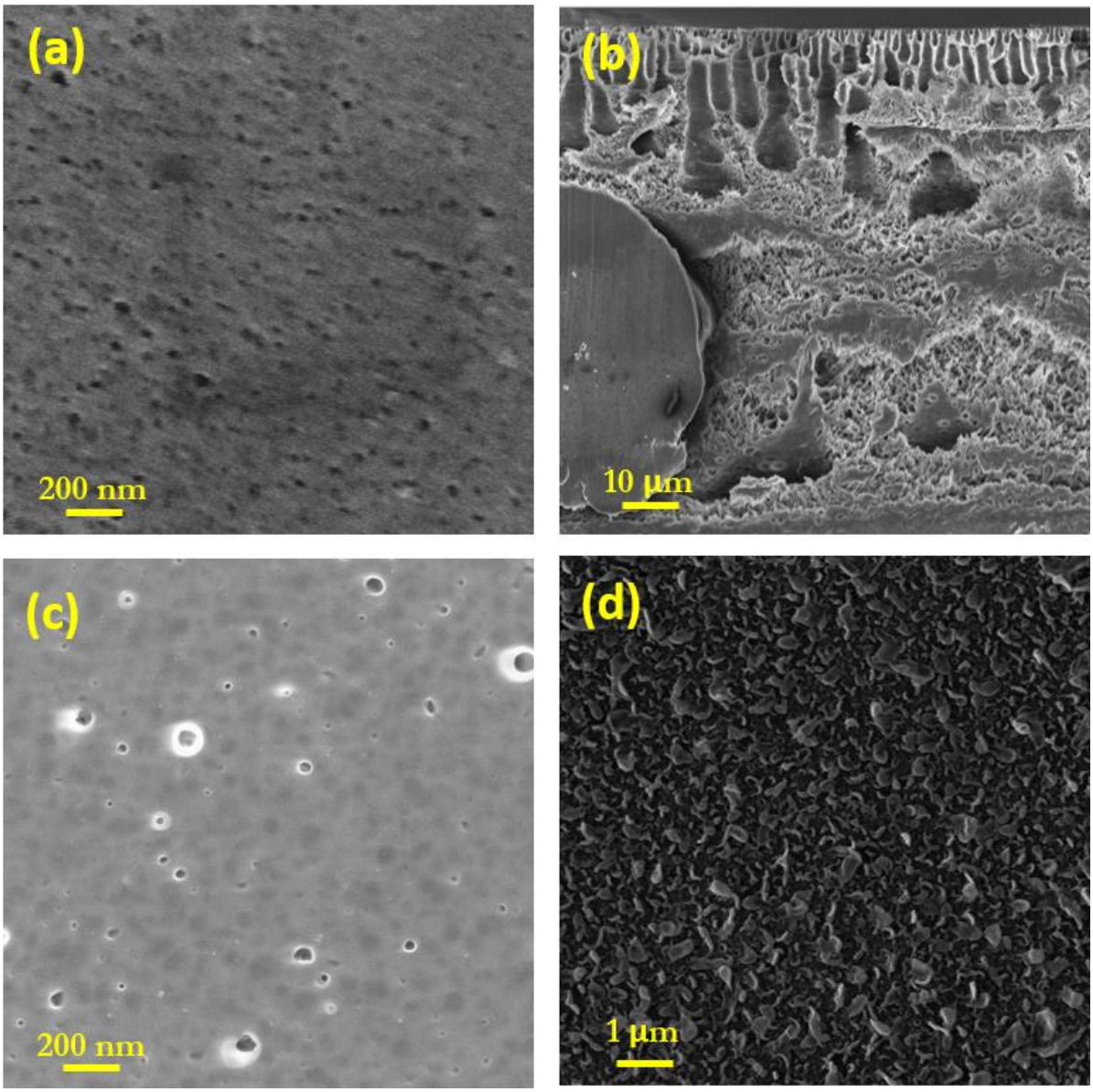


Figure 3. The scanning electron microscope images, showing the morphology of the (a) membrane substrate top surface, (b) membrane cross section, (c) membrane substrate bottom surface, and (d) membrane polyamide active layer surface of a flat sheet TFC PRO membrane.

The first TFC membrane used for PRO application was PA on a polysulfone (PSf) substrate, backed with a polyethylene terephthalate (PET) nonwoven fabric [35]. This membrane has exhibited the suitable morphology for PRO TFC membranes and has become the guideline for succeeding TFC PRO membrane development studies. Polyetherimide (PEi), another commonly-used polymer, was used as the polymeric material in a study which yielded 12.8 W $m^{-2}$ at 17.2 bar using 10 mM NaCl and 1 M NaCl as feed and draw,

respectively [97]. However, deformation of TFC membranes is a huge issue which needs to be addressed during membrane development, such that use of commercial high-mechanical strength polymeric materials and reinforcement of the support layer were performed by a number of PRO TFC membrane researchers. In order to develop a more robust and more mechanically strong membrane, a different class of polymer known as polyimide (PI), more commonly known with trade name Matrimid® 5218, was used for PRO membrane development [98, 99], wherein a porous substrate with sponge-like structure was prepared, and the PA layer was modified with certain agents. Another commercially-available polymer is polyamide-imide (PAI), whose trade name is Torlon®, which was used in PRO membrane studies [100]. Similarly, reinforcement of the PRO TFC supports have been performed in various PRO membrane development studies. She et al. [101] tested different types of fabric as fabric reinforcement materials for PRO TFC membranes, and found that tricot fabric has the best potential for PRO membrane preparation, due to its resistance to tensile stretching, as compared to woven and non-woven fabric, and this TFC membrane exhibited a power density of 7.1 W $m^{-2}$ at 18.4 bar. This has led to further studies which examined the role of reinforcing materials on PRO TFC membrane performance [102, 103].

To improve the mechanical strength, pore structure, hydrophilicity, and functionality of the TFC PRO membranes, chemical modification is essential [104]. A TFC PRO membrane with polyacrylonitrile (PAN) substrate was developed after chemical treatment of the PAN substrate with ethanol [105]. Chemical treatment of the TFC membranes improved the water flux and mechanical stability of the membrane, while it is able to swell the polymeric chains, which results in the formation of a thinner and smoother PA layer with a larger free volume, which led to higher water flux.

In recent, membrane researchers have exploited the properties of functional nano-sized materials to develop nanocomposite membranes with enhanced porosity, hydrophilicity, anti-fouling property, and energy-harnessing capability.

Son et al. incorporated functionalized carbon nanotube (CNT) in the polyethersulfone (PES) support [106]. The CNT effectively increased the membrane porosity, pore size, and hydrophilicity of the TFC membrane. A dual-layered TFC PRO membrane, whose membrane substrate was incorporated with graphene oxide (GO) and halloysite nanotube (HNT) was prepared using a dual-blade casting technique to enhance water flux and antifouling property. The membranes exhibited better fouling mitigation and the membrane with the optimal GO and HNT loading exhibited a power density of 12.1 W $m^{-2}$ at 21 bar using 1.0 M NaCl as draw [85]. A new class of nanomaterials known as covalent organic framework (COF) was also incorporated in the polyamide layer of a PRO thin film nanocomposite (TFN) membrane.

Gonzales et al. [107] synthesized a melamine-based Schiff base network (SNW-1), which was afterwards incorporated in the polyamide layer. After investigating the mode of incorporation and the optimal loading, they reported their best SNW-1-incorporated TFN membrane to have a power density of 12.1 W $m^{-2}$ at 21 bar with DI water as feed and 1 M NaCl as draw.

A recently reported membrane with unprecedented thinness and high water permeability was reported [108]. A fabric support-free PRO TFC membrane was developed using porous polyethylene (PE) separators typically used for lithium-ion battery applications coated with polyvinyl alcohol (PVA) and cross-linked with glutaraldehyde (GA), prior to toluene-assisted IP. The hydrophilized PE battery separators exhibited structural parameter values of around 235 μm. The pure water permeability of the membrane was found to be 8.8 L $m^{-2}$ $h^{-1}$ $bar^{-1}$, which corresponded to the highest reported power density for TFC membranes in literature of 35.7 W $m^{-2}$ at 20 bar.

Table 1 lists the flat sheet-based PRO membranes in literature.

Table 1. Flat-sheet PRO TFC membranes in literature.

| **Membrane substrate** | **Feed solution** | **Draw solution** | **Pressure (bar)** | **Power density (W m-2)** | **Note** | **Reference** |
|---|---|---|---|---|---|---|
| PSf on PET | DI water | 0.5 M NaCl | 12 | 10.0 | PA modified with NaOCl, NaHSO3, heat | [35] |
| PI | DI water | 1.0 M NaCl | 15 | 12.0 | PA modified with NaOCl, NaHSO3, MeOH | [98] |
| PI | DI water | 1.0 M NaCl | 22 | 18.1 | TFC membrane modified with DMF | [99] |
| PAN on PET | DI water | 3.5% (w/w) NaCl | 10 | 2.6 | PAN modified NaOH, HCl; PA modified with NaOCl, NaHSO3, EtOH | [105] |
| PAI on PET | DI water | 3.5% (w/w) NaCl | 13 | 7.1 | PAI was coated with PDA; PA modified with NaOCl, NaHSO3, EtOH | [100] |
| PEi | 10 mM NaCl | 1.0 M NaCl | 17.2 | 12.8 | | [97] |
| PSf on tricot PET | 10 mM NaCl | 1.0 M NaCl | 18.4 | 7.1 | | [101] |
| PES/CNT | DI water | 0.5 M NaCl | 6 | 1.6 | PA modified with NaOCl, NaHSO3, heat | [106] |
| PSf | DI water | 1.0 M NaCl | 22 | 12.9 | | [109] |
| PES on PET | DI water | 1.0 M NaCl | 25 | 12.1 | | [102] |
| PSf/GO and PSf/HNT (dual layer) on PET | DI water | 1.0 M NaCl | 21 | 12.1 | | [85] |
| PK on PET | DI water | 0.6 M NaCl | 28 | 6.1 | | [103] |
| PAI | DI water | 1.0 M NaCl | 21 | 12.1 | PA incorporated with SNW-1 | [107] |
| PVA-coated PE | DI water | 1.0 M NaCl | 20 | 35.7 | PA formed by toluene-assisted IP | [108] |

Another type of flat sheet membranes can be prepared from electrospun polymeric supports. Electrospinning is the application of the polymer solution driven by electrostatic force, forming nano-sized polymer fibers, which are collected on a rotating collector whose electric potential is significantly lower [43]. The nanofiber mat produced after the electrospinning exhibits high porosity and tortuosity [110]. Electrospun nanofiber mats can be used as either the membrane support layer of a TFC membrane or a replacement for the non-woven polyester fabric base. This section focuses on the TFC PRO membrane development studies which used electrospun nanofiber mats for either purpose.

PAN-$SiO_2$ nanofibers were electrospun on a nonwoven PET fabric, prior to active layer formation via IP in the first nanofiber-supported PRO membrane development study [111]. $SiO_2$ was synthesized in the PAN solution before electrospinning via the reaction of tetraethyl orthosilicate (TEOS) and acetic acid. Another set of nanofiber-supported PRO TFC membranes was prepared using PAN on nonwoven PET fabric. Two different kinds of membranes was formed during IP: (1) the typical TFC membrane with PA from the reaction of MPD and TMC; and (2) TFC membrane with PA formed from polyethyleneimine (PEI) and isophthaloyl chloride (IPC) [112]. A tiered nanocomposite membrane support made of polyetherimide (PEi) was reinforced with functionalized carbon nanotubes (CNTs) to deliver a TFC membrane with an outstanding power density of 17.3 W $m^{-2}$ at a pressure of 16.9 bar [113].

A limitation of nanofiber-supported membranes is the poor mechanical strength of the nanofiber substrate, that is why usually a nonwoven backing support is required. Another method in literature which can significantly enhance the robustness and strength of nanofiber-supported membranes is thermal rearrangement of the polymeric material. In three studies, hydroxy polyimide (HPI) nanofibers were electrospun and then placed in a furnace to allow thermal rearrangement to polybenzoxazole-co-imide to occur [114-116]. In one of these studies [116], the nanofibers were also crosslinked to further improve the mechanical strength of the membranes.

Studies involving electrospun nanofiber support for PRO membrane development show the material's applicability; however, its limitation in terms of mechanical strength still exists [117]. During application of high hydraulic pressure during PRO, nanofiber-based membranes are expected to sustain damage. To continue the development of nanofiber-based PRO TFC membranes, it is important to control the structure and use other materials to reinforce the mechanical strength and stability of the membranes.

Table 2 lists the electrospun nanofiber-based PRO membranes in literature.

Table 2. Nanofiber-based PRO TFC membranes in literature.

| Material | Feed solution | Draw solution | Pressure (bar) | Power density (W m-2) | Note | Reference |
|---|---|---|---|---|---|---|
| PAN/SiO2; PET | 0.9 mM NaCl (synthetic river water) | 1.06 M NaCl (synthetic seawater brine) | 15.2 | 10.3 | Substrate coated with PVA; PA modified with NaClO, NaOH | [111] |
| PAN in DMF; PET | DI water | 0.6 M NaCl | 10 | 8.0 | PA formed from MPD and TMC | [112] |
| | | | 8.3 | 6.2 | PA formed from IPC and PEI | |
| PEi/fCNTs | DI water | 1.0 M NaCl | 16.9 | 17.3 | Tiered nanofiber structure | [113] |
| HPI thermally rearranged to PBO | DI water | 1.0 M NaCl | 15 bar | 17.9 | Substrate coated with PDA, NAOH; PA treated with DMF | [114] |
| | | 3.0 M NaCl | 18 bar | 39.5 | | |
| HPI thermally rearranged to PBO | DI water | 3.0 M NaCl | 27 bar | 87.2 | Fluorinated | [115] |
| HPI thermally rearranged to PBO | DI water | 1.0 M NaCl | 21 bar | 26 | Substrate treated with DMSO; PA treated with NaOCl | [116] |

4.2. Hollow fiber TFC PRO membranes

Hollow fiber membranes are self-supporting, tubular shaped membranes which are typically prepared through phase separation spinning process, either via NIPS or thermal induced phase separation (TIPS). During TIPS, the polymer was mixed with a diluent, and is made in contact with a quenching bath at a high temperature. Like NIPS, the diluent and the quenching bath are incompatible with each other and the e separation is heavily influenced by the heat transfer. Hollow fiber membranes are known to have higher surface area compared to flat sheet membranes. This is highly important, especially for productivity and scaling up of the membrane development process and the subsequent commercialization. Furthermore, hollow fiber membranes are known to have better mechanical support and convenience in modulation, as the hollow fiber membrane module can have a high packing density and does not require the use of feed spacers [118-120]. Figure 4 shows the typical morphology of a hollow fiber TFC PRO membrane, whose substrate is prepared via NIPS. The elimination of the use of spacers for hollow fiber membrane modules minimizes the interactions between the membrane and the spacer, as well as the energy loss in the feed flow channel due to these interactions [121].

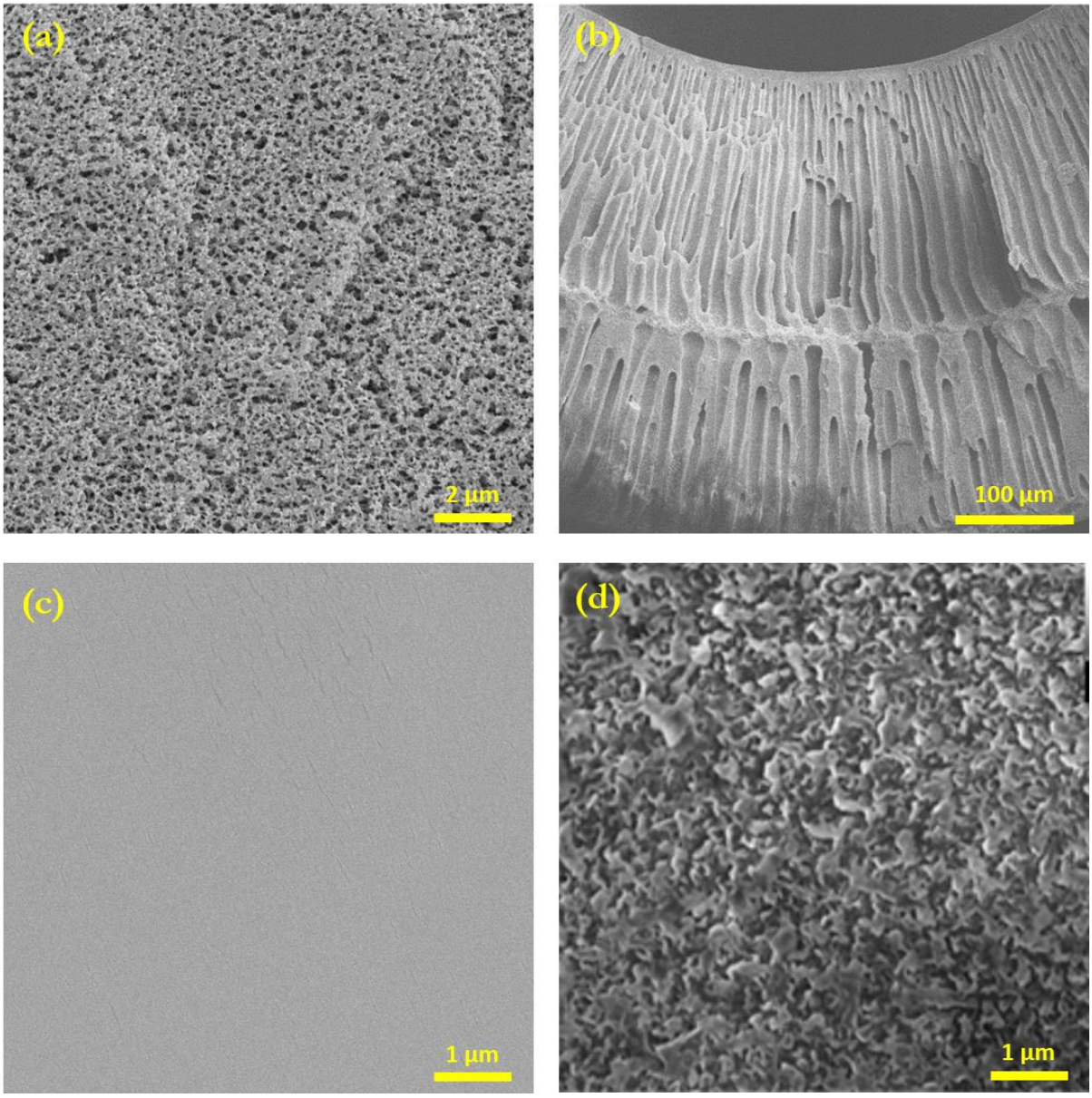


Figure 4. The scanning electron microscope images, showing the morphology of the (a) membrane substrate top surface, (b) membrane cross section, (c) membrane substrate bottom surface, and (d) membrane polyamide active layer surface of a hollow fiber TFC PRO membrane.

During hollow fiber a viscous polymer solution pumped through a spinneret at the same time as a non-solvent bore solution pumped through another tube into the spinneret delivered into a non-solvent coagulation bath. The formed fibers are then collected using a rotary winder. A number of parameters can be controlled during hollow fiber preparation, such as bore and polymer solution flow rate, air residence

time or air gap distance, and take-up rate.

Chou et al. [122] developed the first hollow fiber TFC PRO membrane reported in literature. The PES hollow fiber TFC membrane exhibited a power density of 11 W $m^{-2}$ using synthesized river water and seawater brine as feed and draw, respectively, at 8.4 bar. This membrane suffered from weak mechanical strength, having burst at only 9 bar, so the same group developed hollow fiber membrane using PEI [123]. The resultant membrane had an enhanced mechanical strength, that a maximum power density of 20.9 W $m^{-2}$ was achieved at 15 bar using the same set of FS and DS. PES and PEI were still widely used as the polymer for hollow fiber membranes.

Zhang et al. [124] manipulated the co-extrusion method to prepare a tailored PES hollow fiber membrane support, and the TFC membrane achieved a power density of 24.0 W $m^{-2}$ at 20 bar, using DI water as feed and 1 M NaCl as draw. Other studies continued using PES and PEI hollow fiber substrates for the TFC membranes, all trying to further enhance the membrane properties and performance, as well as modification [125-128].

Ingole et al. [129-131] started fabricating a plain PES hollow fiber TFC PRO membrane, and to improve the performance of the membrane after certain modifications and treatments, like polydopamine (PDA) coating and treatment with tributylphosphate (TBP).

Li et al. used a novel co-polyimide polymer, 3,3',4,4'-benzophenone tetra-carboxylic dianhydride and 80% methylphenylediamine + 20% methylene diamine (BTDA-TDI/MDI) as the membrane substrate material, and the membrane exhibited a power density of 12 W $m^{-2}$ at 21 bar.

Following their initial work with PI flat sheet PRO TFC membranes, researchers from the National

University of Singapore developed PI hollow fiber PRO TFC membranes. Han et al. [132] prepared hollow fiber membranes using PI, which exhibited 16.5 W $m^{-2}$ power density at 15 bar for feed of 10 mM NaCl and draw of 1 M NaCl. The same group also introduced the outer-selective hollow fiber membranes, wherein the polyamide selective layer was formed on the shell side of the fibers. Outer-selective hollow fiber membranes have higher surface area, compared to inner-selective ones; however, these membranes are not easy to make into modules and the IP process usually encounters challenges. Sun et al. [133] employed vacuum-assisted IP to form the active layer on the shell side of PI hollow fiber substrates coated with PDA. The membranes exhibited super mechanical strength, with a burst pressure over 20 bar, and a maximum power density of 7.63 W $m^{-2}$ at 20 bar with DI water and 1 M NaCl, respectively, as feed and draw. Cheng et al. [134] and Le et al. [135] followed a similar approach in fabrication of outer-selective hollow fiber membranes.

Fu et al. conducted two dual-layer hollow fiber PRO TFC studies using polybenzimidazole (PBI). Their first study used PAN as the inner layer material, and a thin outer layer of PBI mixed with polyhedral oligomeric silsesquioxane (POSS), to prevent the PBI from delaminating, prepared via co-extrusion [136]. This membrane exhibited 2.5 W $m^{-2}$ at 7 bar using 1.0 M NaCl as draw. This first study on dual-layer hollow fiber membranes yielded low flux due to the macromolecular additive PVP entrapped within the inner layer. A second study tried to correct this by subjecting the membranes into ammonium persulfate (APS) treatment to remove the PVP and improve the water permeability of the membranes. After treating the dual layer PAN and PBI/POSS hollow fiber with APS, the maximum power density was improved to 5.1 W $m^{-2}$ at 15 bar. A TFC membrane with double polyamide layer was prepared by Han et al. [87] to mitigate both ICP and fouling, with the membranes exhibiting 10.7 W $m^{-2}$ at 15 bar with 1 M NaCl and DI water as draw and feed, respectively.

Chemically modified hollow fiber TFC PRO membrane were developed in several studies. Li et al. [80]

grafted hyperbranched polyglycerol (HPG) onto a PES hollow fiber substrate, prior to IP. This membrane, with enhanced antifouling capability, exhibited a power density of 6.7 W $m^{-2}$ at 16 bar with 3.5% NaCl as draw against DI water as feed. Sulfonate hyperbranched polyglycerol Grafting of aminosilane, specifically 3-aminopropyltrimethoxysilane (APTMS), was also performed by Zhang et al. [78] to improve the fouling resistance of the membrane.

Municipal wastewater was used as the FS in a study of Zhao et al. [75] wherein they prepared antifouling membranes modified with zwitterionic 2-methacryloyloxyethylphosphorylcholine (MPC) which exhibited 7.7 W $m^{-2}$ power density at 15 bar. MPC was then reacted with 2-aminoethyl methacrylate hydrochloride (AEMA) via a single-step free radical polymerization to synthesize the P[MPC-co-AEMA] copolymer, which was grafted on a hollow fiber substrate made from blend of PES and PAI, and the membrane exhibited a power density of 13.5 W $m^{-2}$ at 20 bar [76]. Li et al. exploited the properties of poly(allylamine hydrochloride) (PAH) to modify TFC PRO membranes. First, they used layer-by-layer (LbL) polyelectrolyte deposition of PAH and poly(acrylic acid) [74]. Another study involved the crosslinking of PAH onto the surface of the PAI hollow fiber substrate using glutaraldehyde (GA).

Nanocomposite hollow fiber membranes were also prepared via the incorporation of nanomaterials. Zhao et al. [82] grafted carbon quantum dots (CQDs) on PDA-coated PES hollow fiber membranes and achieved a power density of 11.0 W $m^{-2}$ at 15 bar. CQDs were then incorporated in the selective polyamide layer of PRO hollow fiber TFN membranes by Gai et al. [137] exhibiting 34.2 W $m^{-2}$ power density at 23 bar. GO was then mixed by Park et al. [138] in PES hollow fiber substrate to prepare a TFC membrane with 14.6 W $m^{-2}$ power density at 16.5 bar.

Thermally-assisted nonsolvent-induced phase separation (T-NIPS) was introduced by Cho et al. [139] to tailor the structure of a CTA/CA hollow fiber membrane with a dense outer layer and isoporous inner

layer.

Following their earlier work in nano-sized material-incorporated TFN membranes, Gonzales et al. [140] synthesized sulfonate- functionalized porous organic polymer, PP-$SO_3H$, and incorporated this polymer in a hollow fiber TFC membrane with a power density of 14.6 W $m^{-2}$ at 17 bar.

Table 3 lists the hollow fiber-based PRO membranes in literature.

Table 3. Hollow fiber PRO TFC membranes in literature.

| Membrane substrate | Active layer | Feed solution | Draw solution | Pressure (bar) | Power density (W m-2) | Note | Reference |
|---|---|---|---|---|---|---|---|
| PES | PA on lumen side | 10 mM NaCl | 1.0 M NaCl | 9 | 10.6 | | [122] |
| PEI | PA on lumen side | 10 mM NaCl | 1.0 M NaCl | 15 | 20.9 | | [123] |
| PAN (inner layer) | PBI/POSS (outer layer) | 10 mM NaCl | 1.0 M NaCl | 7 | 2.5 | Fibers treated with thermal annealing | [136] |
| PAN (inner layer) | PBI/POSS (outer layer) | 10 mM NaCl | 1.0 M NaCl | 15 | 5.1 | Fibers treated with APS | [141] |
| PI | PA on lumen side | 10 mM NaCl | 1.0 M NaCl | 15 | 16.5 | | [132] |
| PI | PA on shell side (outer-selective) | DI water | 1.0 M NaCl | 20 | 7.6 | PDA intermediate layer was formed | [133] |
| PES | PA on lumen side | DI water | 0.6 M NaCl | 6 | 1.5 | | [129] |
| PES | PA on lumen side | DI water | 0.6 M NaCl | 7 | 3.0 | PDA intermediate layer was formed | [130] |
| PES | PA on lumen side | DI water | 0.6 M NaCl | 8 | 3.9 | PDA intermediate layer was formed; PA treated with TBP | [131] |
| PES | PA on lumen side | DI water | 3.5% (w/w) NaCl | 16 | 6.7 | PDA-coated support grafted with HPG | [80] |
| PES | PA on lumen | Wastewater retentate | 0.81 M NaCl | 20 | 18.8 | PDA-coated Support grafted with | [79] |

| | | | | | | | |
|---|---|---|---|---|---|---|---|
| | side | | | | | SHPG, TEA | |
| BTDA-TDI/MDI | PA on lumen side | DI water | 1.0 M NaCl | 21 | 12 | | [142] |
| PES | PA on lumen side | DI water | 1.0 M NaCl | 24 | 21 | | [124] |
| PES | PA on shell side (outer-selective) | DI water | 1.0 M NaCl | 20 | 7.8 | | [134] |
| PES | PA on lumen side | DI water | 1.0 M NaCl | 20 | 22.1 | | [125] |
| PES | PA on lumen side | DI water | 1.0 M NaCl | 22 | 10.1 | | [126] |
| PES | PA on lumen side | DI water | 1.0 M NaCl | 20 | 22.0 | | [127] |
| PES | PA on lumen side | DI water | 1.2 M NaCl | 30 | 38 | | [143] |
| PEI | PA on lumen side | DI water | 1.0 M NaCl | 15 | 8.9 | | [128] |
| PEI | PA on shell side (outer-selective) | DI water | 1.0 M NaCl | 17 | 9.6 | | [135] |
| PEI | PA on shell side (outer-selective) | DI water | 1.0 M NaCl | 13 | 13 | Modified with APTMS | [78] |
| PES | PA on shell side (outer-selective) | Municipal wastewater | 0.81 M NaCl | 15 | 7.7 | Substrate modified with PDA and MPC | [75] |
| PES | PA on both | DI water | 1.0 M NaCl | 15 | 10.7 | Dual selective layer | [87] |

| | | | | | | | | |
|---|---|---|---|---|---|---|---|---|
| | sides (dual layer) | | | | | | | |
| PEI | PA on lumen side | DI water | | 1.0 M NaCl | 15 | 16.2 | LbL deposition of PAH and PAA on substrate | [74] |
| PES | PA on lumen side | DI water | | 0.81 M NaCl | 15 | 11 | CQDs grafted on shell side | [82] |
| PES | PA on lumen side | DI water | | 1.0 M NaCl | 23 | 34.2 | CQDs incorporated in PA layer | [137] |
| PES/GO | PA on lumen side | DI water | | 1.0 M NaCl | 16.5 | 14.6 | | [138] |
| PES/PAI | PA on lumen side | DI water | | 1.0 M NaCl | 20 | 13.5 | Substrate modified with P[MPC-co-AEMA]c | [76] |
| PAI | PA on lumen side | Wastewater retentate | RO | 1.0 M NaCl | 13 | 4.3 | Substrate modified with crosslinking of PAH, GA | [144] |
| CTA/CA | - | DI water | | 1.0 M NaCl | 18 | 5.5 | Hollow fiber fabricated using T-NIPS | [139] |
| PES | PA on lumen side | DI water | | 1.0 M NaCl | 17 | 14.6 | Porous polymer PP-$SO_3H$ incorporated in PA layer | [140] |

4.3. Free-standing PRO membranes

To minimize the occurrence of ICP during PRO operations, a new class of membranes were being developed, known as free-standing membranes. These membranes eliminate the use of membrane substrate or support layer to be able to achieve high water flux. The first reported free-standing membrane was reported by Patel et al. [145]. A poly(vinyl chloride)-g-poly(3-sulfopropyl methacrylate) graft copolymer was synthesized and cast using NIPS, similar to flat-sheet membrane substrates. This membrane was able to generate 0.88 W $m^{-2}$ power density at 14 bar using model seawater as draw. Tong et al. [146] prepared free-standing GO membranes for PRO, wherein GO sheets were filtered onto an inorganic porous filter. Using 3 M NaCl and 0.017 M NaCl as draw and feed, respectively, a power density of 24.62 W $m^{-2}$ was achieved at an applied pressure of 6.90 bar. Following this study, Gao et al. [147] mixed together GO and two-dimensional MXene $Ti_3C_2T_x$ material to prepare the freestanding membrane which was able to achieve a power density of 56.4 W $m^{-2}$ at 9.66 bar using 2.0 M NaCl as draw and 0.017 M NaCl as feed.

While the development of free-standing membranes seems attractive due to the high power density and water flux values achieved, the ability of these membranes to sustain hydraulic pressure application has yet to be optimized, since elimination of the membrane substrate significantly affects the mechanical strength and stability of the membranes. Moreover, the free-standing membranes in literature used nanomaterials, which may not be the most economical choice for membrane materials, and, thus, can affect the larger-scale development of these membranes.

## 5. Module development for pressure retarded osmosis

A number of PRO studies have expressed concern for problematic module, spacer designs, and membrane fouling which were found to significantly affect the membrane integrity, process performance and efficiency [148-150]. Initially, RO modules were used for PRO studies due to the similarity in use of applied hydraulic pressure; however, due to the basic differences between the two processes, RO modules were found to be not-suitable for PRO [40]. RO only has feed circulation on one side, whereas PRO requires simultaneous

feed and draw circulation, thus the PRO module should be able to maximize flow and circulation efficiency, while being able to mitigate fouling tendency [128, 150]. FO modules were then tested due to the availability of four ports for inlet and outlet of feed and draw streams; however, most FO modules could not sustain the hydraulic pressure applied during PRO operation.

### 5.1. PRO module development

Due to the pressure tolerance requirements of the PRO process, PRO membrane modules are only limited to either spiral-wound module for flat sheet membranes or hollow fiber membrane module. Figure 5 shows a representation of these membrane module configurations. Module-scale PRO studies, thus far, could not achieve the performance of bench-scale PRO experiments, mainly due to the membrane module hydrodynamics and inconsistency in pressure and osmotic driving force distribution inside the module, as well as the inevitable dilution of the DS [151].

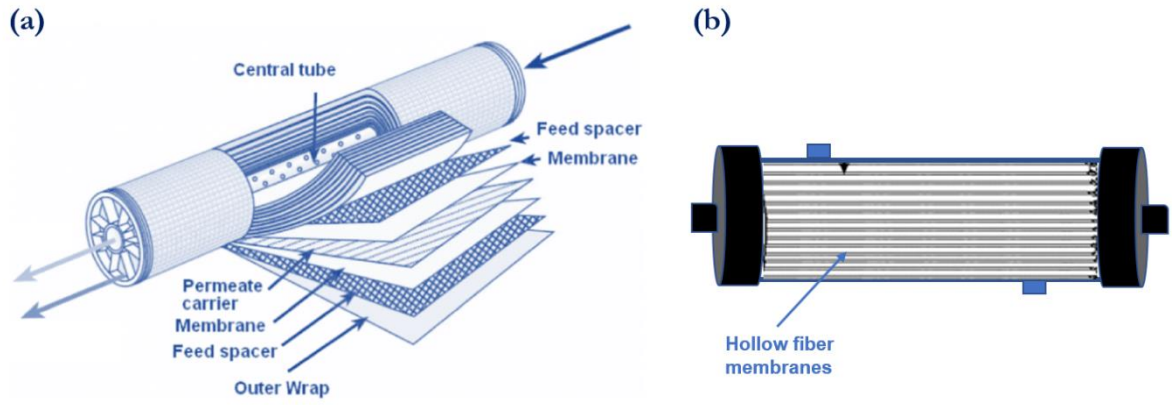


Figure 5. Representations of the commercial membrane modules for PRO: (a) spiral-wound and (b) hollow fiber.

One of the modular configurations for TFC membranes is the spiral-wound module, which can be applied for flat-sheet membranes. The spiral-wound module is the preferred membrane module configurations for

flat sheet PRO membranes. The spiral-wound module is composed of membrane sheets placed in between spacers housed in a module casing. The membrane sheets are glued together with spacers in between each sheet to form a leaf. The leaves are afterwards rolled around to form feed and draw solution channels inside the membrane module. Spiral-wound modules are suitable for flat sheet membranes due to high packing density which could be achieved from this configuration, compared with other flat sheet module configurations. A challenge in the development of spiral-wound modules for PRO is the loss of pressure inside the membrane module, due to the feed channel spacers, which are designed to enhance mass transfer within the module [152]. Furthermore, this module configuration requires suitable spacers for PRO operation. The spiral-wound configuration can be used for most osmotic processes; however, for PRO implementation, the spacer design of conventional spiral-wound modules was found to be not suitable, as the spacers could cause membrane damage and pressure drop. Kim et al. [151] operated an HTI PRO using a spiral-wound module with two different flow paths, axial and spiral, and two different spacers, net-type for the draw stream and tricot for the feed stream. Toray Chemicals, a textile and polymer manufacturing company, also came up with a PRO TFC spiral-wound module, which was used for the GMVP project in Korea. Due to these efforts, module development for PRO has continued to advance.

On the other hand, hollow fiber modules are composed of hollow fibers bundled and housed together in a compact housing, with surface-to-volume ratios and packing densities higher than that of the spiral-wound module. Other advantages of hollow fiber modules include strong pressure resistance with proper and consistent flow distribution within the module [153]. During one PRO module study, a pilot CTA hollow fiber module for PRO was evaluated for performance and use for PRO [154]; but since then, TFC PRO hollow fiber membranes have posed problems regarding modulation and membrane creeping [155]. The biggest challenge in the development of hollow fiber modules is the optimization of the quantity of the hollow fibers and the suitable potting process to prepare the membrane modules with minimal defects. Defects in the PRO module could result in membrane creeping and membrane bursts during higher

pressure operation. Another limitation of the hollow fiber module is the pressure tolerance, as feed and draw pressures are usually limited for this module type. Following this PRO hollow fiber module work, a number of modulation studies to solve the perceived modulation problems and provide outstanding water and solute transport mechanisms.

Sivertsen et al. simulated various configurations of hollow fiber modules for PRO application, and found that overall PRO performance was similar regardless the module configuration [120] and the thermodynamics and mass transfer in hollow fiber modules were simulated by Xiong et al. [156]. Commercialization of hollow fiber modulation for PRO, however, has still not progressed significantly, albeit with a number of laboratory-scale studies [127, 128]. In fact, commercialization of hollow fiber membranes for PRO has only been achieved by Japanese company Toyobo, whose PRO hollow fiber modules were used for the Mega-ton project in Japan. Table 4 lists the performance of commercial PRO membranes in literature.

### 5.2. PRO spacer development

In the same manner, spacer development for PRO has not reached any significant milestone. Spacer development for a specific process is important as it is able to influence not only the operational efficiency, but the membrane lifetime as well. With the use of non-suitable spacers, membrane deformation and damage could possibly occur, affecting membrane performance and often leading to membrane collapse [88, 148]. It was observed that the application of high hydraulic pressure on the draw stream could cause membrane deformation due to the use of feed channel spacer [149]. This led to the assessment of different types of spacers suitable for use with PRO membranes.

In addition, fouling of the PRO membranes is a major hurdle affecting the PRO process efficiency, as not only antifouling membranes may reduce fouling but also as pre-treatment processes are another focus in the PRO research [157]. Less fouling propensity can make the PRO process more workable when using

wastewater concentrate FS. The integration of PRO process with another desalination technology shows advantages over the individual PRO system. This is because the diluted FS is supplied to the PRO process and the PRO membrane becomes less fouled as a result of low salinity and foulants in the FS. Conventional membrane technology processes are commonly used over the years and there is an urgent need to utilize state of the art pretreatment processes replacing the classical methods.

Table 4. The commercial PRO membrane modules in literature.

| **Company** | **Module type** | **Draw solution** | **Operating pressure (bar)** | **Power density (W m$^{-2}$)** | **Reference** |
|---|---|---|---|---|---|
| Flat-sheet | | | | | |
| HTI | OsMem™ 2521 spiral wound | 0.52 M NaCl | 4.0 | 0.57 | [158] |
| | | 1.03 M NaCl | | 1.10 | |
| | | 0.60 M NaCl | 9.8 | 1.10 | [151] |
| | | 1.03 M NaCl | 4.0 | 3.29 | [88] |
| Toray Chemical Korea | 8040 spiral wound | 0.60 M NaCl | 10.4 | 1.77 | [159] |
| Hollow fiber | | | | | |
| Toyobo | 5 inch | 1.0 M NaCl | 30 | 17.1 | [160] |
| | | 1.0 M NaCl | | 13.3 | |
| | 10 inch | 1.0 M NaCl | 25 | 7.7 | [161] |
| | | 1.0 M NaCl | 29 | 4.4 | |

## 6. Integration of pressure retarded osmosis with membrane pretreatment techniques

PRO is highly versatile process, since a wide variety of possible DS and FS can be exploited to achieve the necessary salinity gradient required for osmotic power generation. This has led to the use of freshwater, wastewater effluent, and pretreated seawater as feed, and seawater and concentrated brine as draw. As a result of the perceived versatility of PRO and the questions on feasibility of PRO as a stand-alone process, PRO was integrated with other membrane-based technologies to be able to exploit high salinity concentrations of byproducts (i.e., brine), augment energy and operational costs, and mitigate environmental impact of direct ocean discharge [162, 163]. Soon, the PRO research community found that hybrid processes involving PRO and conventional desalination processes, such as RO and FO, have great potential, and thus, recently, the direction of PRO research has significantly shifted to hybrid processes. While desalination processes, such as seawater reverse osmosis (SWRO), have already been commercialized or applied at a larger scale, these processes are concerned more about the production of freshwater at a higher efficiency and production rate. In doing this, operational cost and energy expenditure are likewise increasing. This is where PRO can be integrated, as it is a process which is able to perform desalination, but more importantly, at the same time, reduce the energy consumption through power generation [162, 164].

### 6.1. Reverse osmosis and pressure retarded osmosis hybrid

Integration of SWRO and PRO mainly aims to lessen energy expenditure and operating costs, and there are two mechanisms through which SWRO-PRO hybrid systems can achieve this: (1) generation of power through a hydro-turbine, and (2) circulation of energy through a pressure-exchanger. The former has a low energy generation efficiency; however, the electricity produced from this system can also be used for other purpose, not just to provide energy for the desalination plant. Inversely, the use of pressure-exchanger is highly efficient, but the energy or pressure recovered through this mechanism can only be used to augment the energy requirements of SWRO [165]. The pressure recovered through the pressure exchanger is provided to the seawater influent, thus less energy could be used for pressurize the stream.

The most notable integrated PRO hybrid process was Japan's Mega-ton Water System, which integrated SWRO and PRO and whose schematic is shown in Figure 6. For this hybrid installation, SWRO brine from a desalination plant and wastewater effluent from a regional sewage treatment facility were used as draw and feed, respectively, and 10-inch Toyobo CTA PRO hollow fiber modules were used [161, 166]. This SWRO-PRO prototype power plant was able to achieve 13.8 W $m^{-2}$ power density at 30 bar applied hydraulic pressure. In this system, which aimed to produce energy through a turbine and to circulate energy, there were four open ports situated in the PRO hollow fiber module, to provide passage for the feed inlet, draw inlet, permeate outlet, and feed water discharge directed to the effluent tank. The feed water discharge was placed to provide circulation for the feed and mitigate the presence of leaked solute and the occurrence of ICP. During operation, the maximum power density was found to be 13.3 W $m^{-2}$ and energy savings of 10-30% [167].

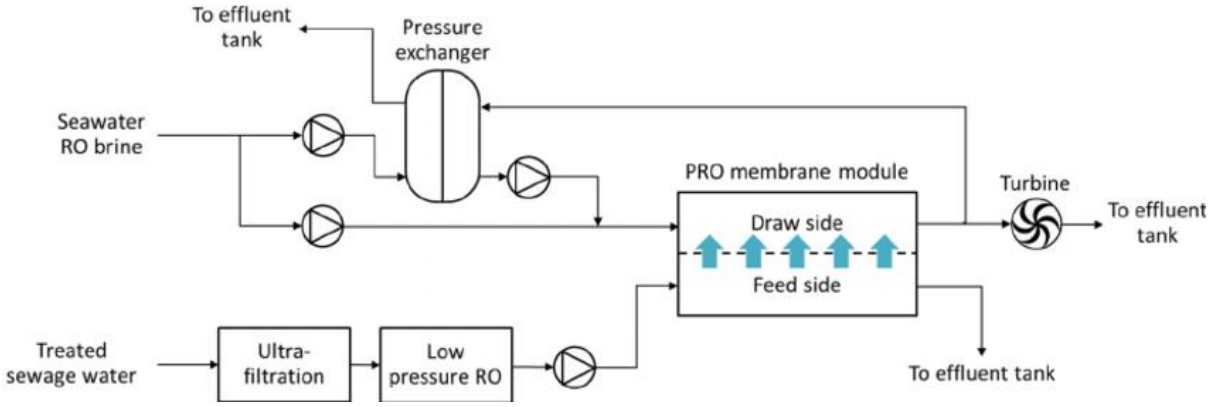


Figure 6. The conceptual schematic of the integrated Mega-ton RO-PRO hybrid system [167, 168].

Following the halt in operations of Mega-ton, the GMVP project continued the large-scale implementation of the PRO hybrid processes. Wastewater treatment plant effluent and SWRO brine were used to achieve a low-cost seawater desalination operation [169]. Instead of focusing on just energy production, GMVP also aimed to recover the pressure from the pressurized DS to augment the pressure demand of seawater

desalination. Osmotic power was generated and recovered using a hydraulic turbine and an energy recovery device (ERD), as shown in Figure 7. The SWRO-PRO demonstration plant was able to treat 240 $m^3$ $d^{-1}$ of seawater. The maximum power density for this implementation was 18.3 W $m^{-2}$ and the energy expenditure was reduced to 80%.

Kim et al. [170] assessed the efficiency of four different configurations of the hybrid RO-PRO system, as shown in Figure 7, which all aimed to focus more on either power generation or fresh water production.

Achilli et al. [171] installed and operated a pilot-scale RO-PRO system using three spiral-wound RO modules connected in series, delivering concentrated seawater brine to an ERD to reduce the pressure prior to use as the draw for the PRO system with a spiral-wound PRO module. Seawater was first pressurized using a pressure exchanger, delivered to the first RO module, and the concentrated seawater brine from each module was used as the feed for the succeeding module, until the brine reaches the ERD and used as draw for PRO, with wastewater effluent as feed. This particular configuration of the integrated RO-PRO system was able to demonstrate efficient energy production and energy consumption, as the seawater brine generated during RO was then diluted back to seawater concentration during PRO, and thus can be reused.

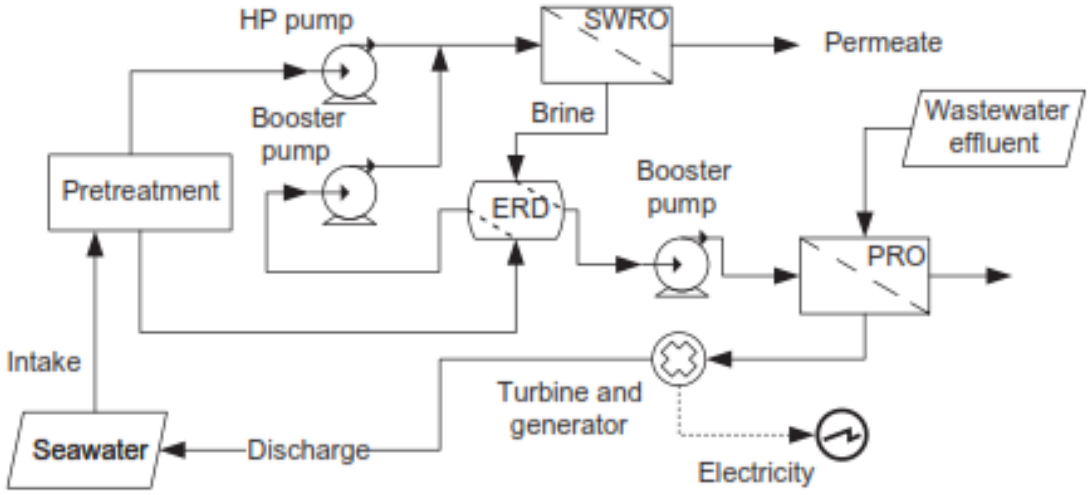


Figure 7. Schematic of four proposed RO-PRO hybrid system configurations [170].

Altaee et al. [172] proposed an integrated power generation and seawater desalination process, wherein PRO was first operated to generate energy using seawater as draw and low-quality water as feed. The diluted seawater was then delivered into a turbine, and afterwards to the RO module for desalination. There are several other studies conducted to investigate and determine the feasibility of the RO-PRO hybrid process, aiming to reduce the specific energy consumption [173, 174], maximize the profit from commercial operation [175, 176], and optimize the process performance [177].

A combined integrated system involving PRO, RO, and nanofiltration (NF) was proposed by Touati et al. [178]. As shown in Figure 8, wastewater effluent was first pretreated using NF, and the permeate proceeded to the PRO system to be used as feed. Seawater, on the other hand, passed through RO operation first and the concentrated brine was used as draw. The treated water in this hybrid system can be used for irrigation, thus this particular system has shown the potential of a combined water treatment, seawater desalination, and energy production to augment requirements for food-water-energy nexus.

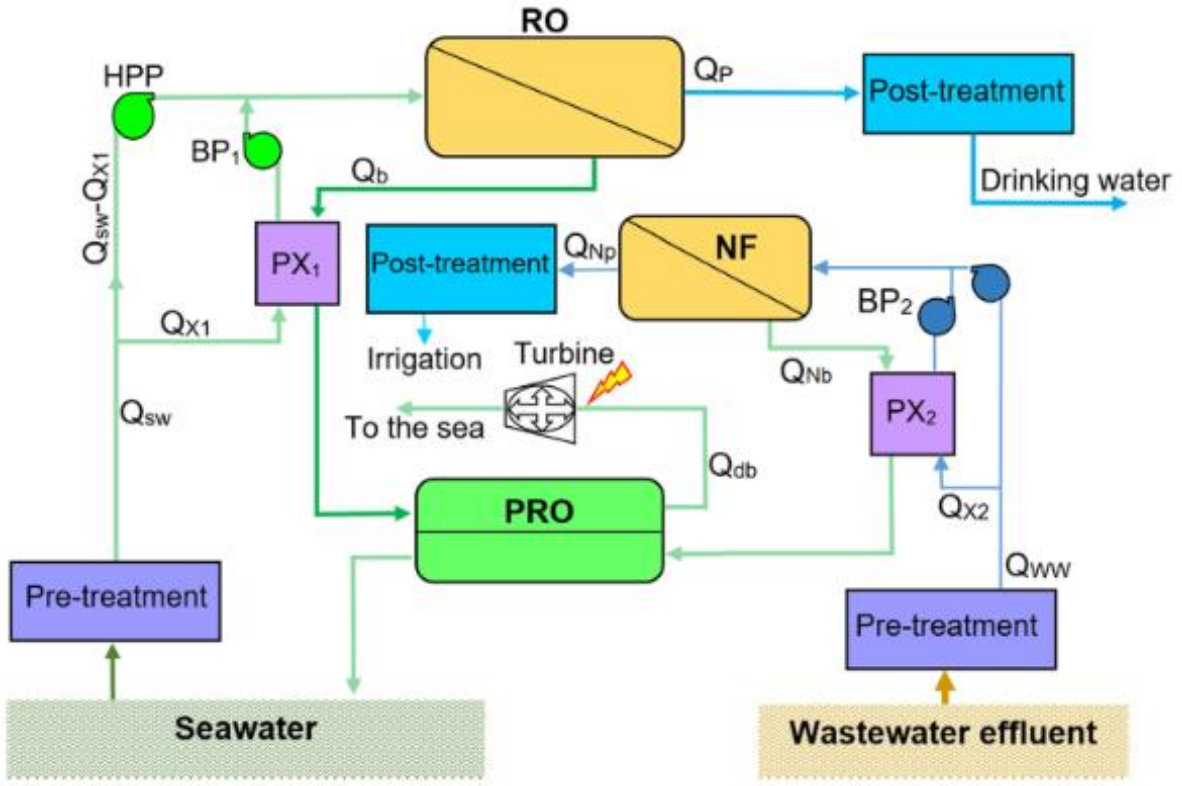


Figure 8. The proposed combined water treatment, seawater desalination, and energy production RO-NF-PRO hybrid process [178].

6.2. Forward osmosis and pressure retarded osmosis hybrid

Two configurations of PRO integrated with FO- PRO-FO and FO-PRO -were evaluated in a previous study [163]. Two similar modules were installed, which both could perform either FO or PRO depending on the configuration, and treated hypersaline solution and wastewater effluent as draw and feed, respectively. An integrated process wherein PRO was operated first followed by FO proved to be more efficient in terms of power generation. Integrated FO-PRO was also conducted by Cheng et al. [179] to mitigate membrane fouling during PRO. The use of real wastewater effluent as FS for PRO posed problems regarding membrane fouling, thus FO was first conducted as a pretreatment step to exploit the several advantages of the FO process: low fouling propensity, simple membrane cleaning strategies, and minimum energy requirement.

PRO was also proposed to be integrated with a biological wastewater treatment process [180]. Wastewater

was first treated by the membrane bioreactor (MBR) and the effluent was used as the feed for PRO. While this system suffered from severe fouling, simultaneous contaminant removal from the wastewater and power production were achieved in this study.

### 6.3. Membrane distillation and pressure retarded osmosis hybrid

PRO was integrated with membrane distillation (MD) in a study conducted by Han et al [181]. PRO was first conducted and the diluted DS after PRO operation was used for MD. This configuration was found to have a high water recovery rate and osmotic power, with minimal membrane fouling.

Lee et al. [182] proposed an integrated vacuum MD (VMD) and PRO system. This system is consisted of a recycling flow VMD scheme operated for continuous production of fresh water and concentrated brine, which was then used as the draw for PRO, as shown in Figure 9.

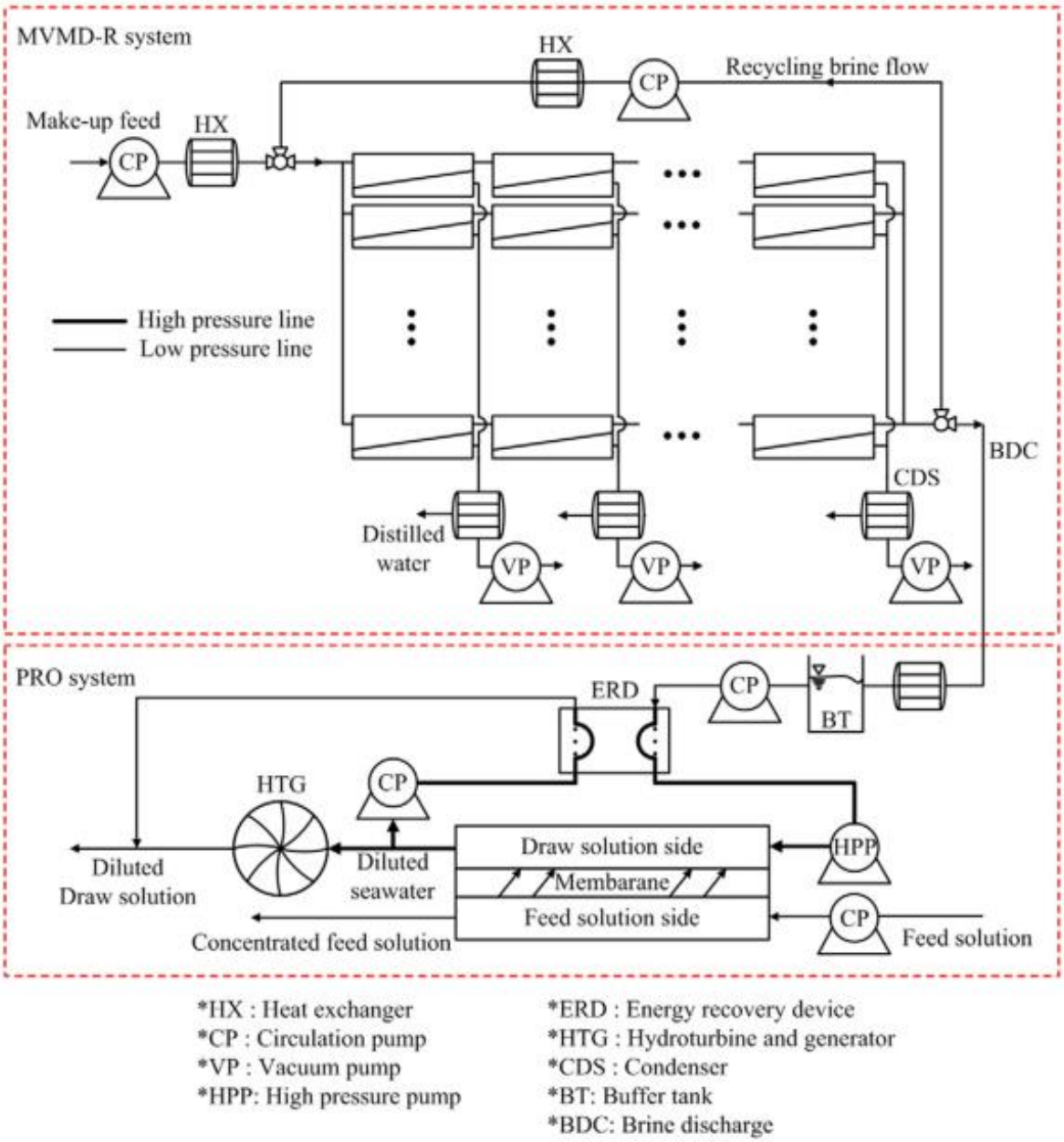


Figure 9. The schematic of the proposed integrated VMD-PRO process [182].

6.4. Liquid phase ion stripping and pressure retarded osmosis hybrid

A new concept of an integrated process involving PRO was introduced by Wang et al. [183]. Liquid-phase ion-stripping (LIS) was used to generate salinity gradient with only low temperature and integrated with PRO. As shown in Figure 10, the saline solution undergoes a thermal cycle, and with organic solvent, ions are rejected to produce fresh water and concentrated brine, which respectively become the feed and draw

for PRO. This proposed hybrid process was found to have high energy efficiency, solvent extraction efficiency, and heat recovery system efficiency.

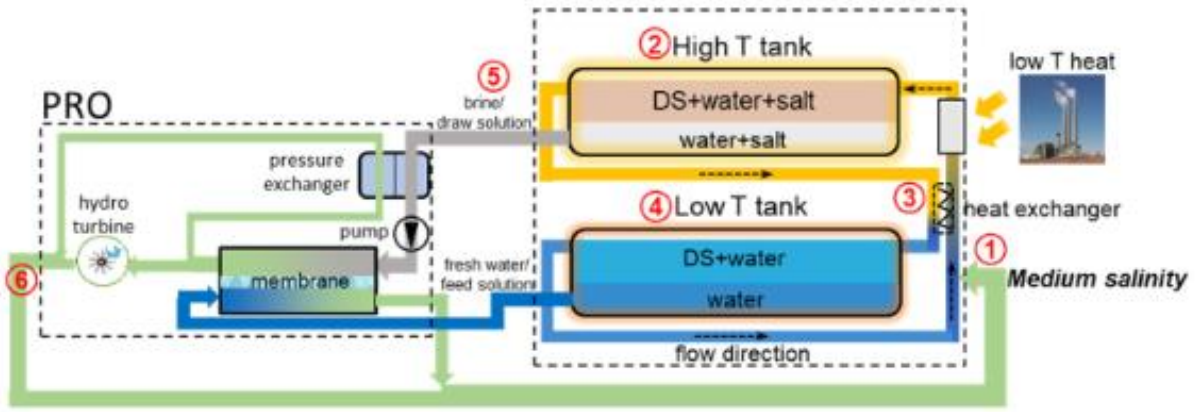


Figure 10. The proposed integrated LIS-PRO hybrid system [183].

## 7. Novel configurations and niche applications of pressure retarded osmosis

Following the versatility of PRO in terms of configuration and DS and FS choice, novel configurations and niche applications of PRO have been proposed and gained attention in recent.

### 7.1. Closed-loop osmotic heat engine

The concept of a closed-loop OHE was first introduced and patented by Sidney Loeb in 1975 [184], but it is not until three decades after when PRO researchers started assessing its feasibility and performance. Hickenbottom et al. [185] exploited the concept of OHE, that is the coupling of PRO with a thermal separation process, i.e., MD. They pointed out that this process will only work when the PRO process is able to achieve high power density, to minimize operational and capital costs, while the MD process must have high water flux to be able to reconcentrate the diluted DS better. Various inorganic and ionic organic DS were tested and assessed in terms of PRO and MD performance, as well as equipment corrosion potential. McGinnis et al. [186] then tried a novel DS for their own application of the closed-loop OHE. Concentrated ammonia-carbon dioxide (from the mixing of $NH_4HCO_3$ and $NH_4OH$) was chosen and used

as the DS, with DI water as the feed. Heat was introduced to the engine to separate the draw solute from the fresh water. The use of the combination of DS and FS allowed lower temperature for draw and feed separation, while using high concentrations of the draw ensured high power density.

To further enhance thermal separation efficiency, DS prepared with an organic solvent were used in an OHE demonstration of Shaulsky et al. [187]. LiCl was chosen as a draw solute and it was mixed in methanol, to exploit the high volatility and lower heat capacity of this particular organic solvent during the MD draw solute reconcentration. Operation using a DS of 3 M LiCl in methanol yielded water flux of 47.1 L $m^{-2}$ $h^{-1}$ and power density of 72.1 W $m^{-2}$, with high heat recovery and energy efficiency.

Another configuration of a closed loop OHE was proposed to utilize low-grade thermal energy using MD coupled with PRO [188]. Using different heat source temperatures and working DS concentrations, energy efficiency was assessed and the process with optimized, and it was found out that at lower working temperatures of 60 and 20 ºC, use of a higher working concentration of draw would enhance the process efficiency. Instead of MD, multi-effect distillation (MED) was performed for thermal separation in the OHE process proposed by Altaee et al. [189]. They proposed two different configurations of the OHE: a single stage conventional OHE, and the dual-stage closed-loop process. MED was chosen due to the deemed free source of waste heat utilizable for thermal regeneration. With their simulation, they were able to show that dual-stage closed loop PRO was 20% more efficient than the single-stage OHE.

### 7.2. Dual-stage PRO

Among the earlier novel configurations of PRO is the installation of a dual-stage PRO system. Introduced in 2014 by Altaee et al. [190], the dual-stage PRO process aimed to utilize two different feed streams: brackish/fresh water and wastewater, as shown in Figure 11. The feed streams were delivered separately into the PRO modules, with the pressurized seawater delivered continuously into the two PRO modules in series. The diluted DS recovered after the second stage PRO treatment was depressurized by a turbine for

power generation. This configuration was found to generate higher power density; however, capital costs of the system were also significantly higher due to the employment of two PRO modules. Following the results of the first study, the dual-stage PRO process was then further optimized to enhance process performance, leading to the proposition of a new design configurations of the dual-stage PRO process, also shown in **Error! Reference source not found.**. In the old configuration, the diluted DS from the first stage was delivered onto the second stage; in the modified configuration, the seawater flow goes from the first stage to the second stage simultaneously from the pressurized DS chamber. This configuration significantly improved the PRO performance, due to the higher water flux obtained at the second stage.

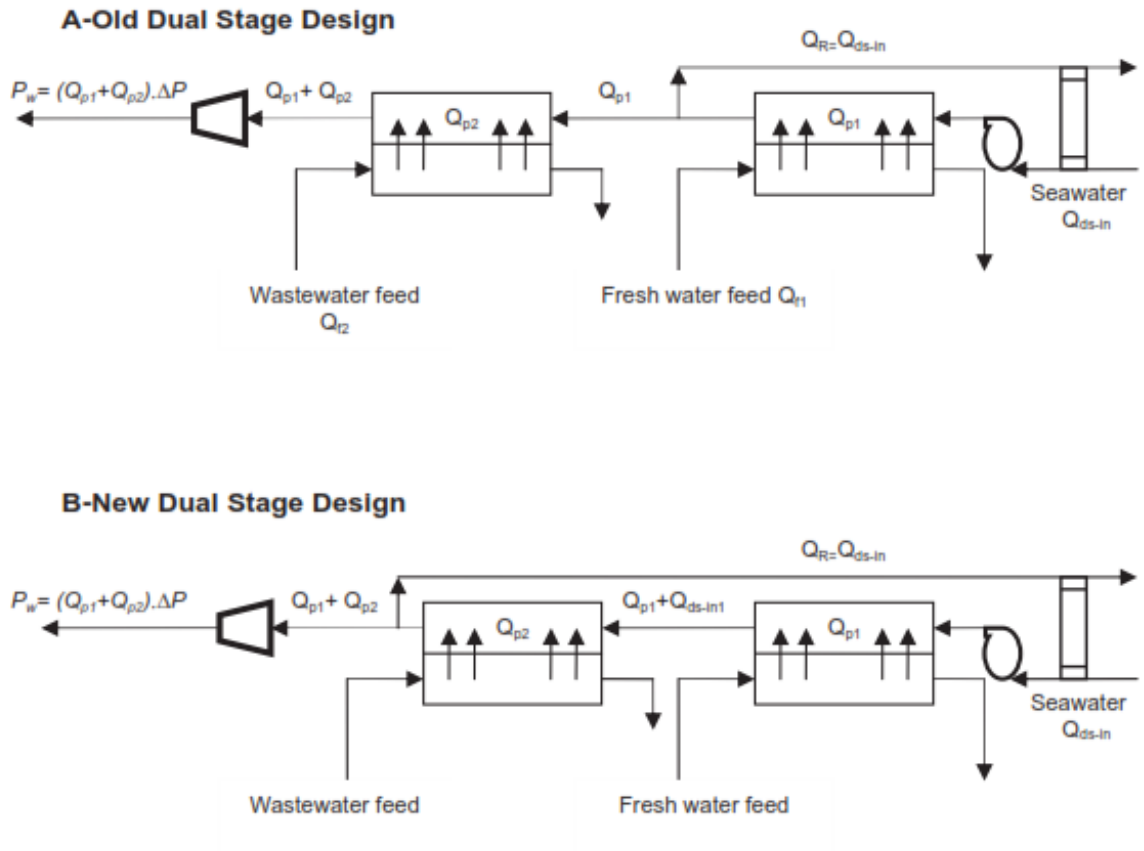


Figure 11. The conceptual schematic of dual-stage PRO operation using two different feed streams: (a) first configuration [190] and (b) second configuration.

Another group proposed the enhanced energy recovery using a two-stage PRO system. He et al. [191] proposed four different configurations of the dual-stage PRO system, as shown in Figure 12: (a) continuous

draw and feed (CDCF); (b) divided draw and continuous feed (DDCF); (c) continuous draw and divided feed (CDDF); and (d) divided draw and feed (DDDF). For CDCF, the draw and feed streams are connected in series through two PRO modules. DDDF, on the other hand, delivers draw and feed from the same source tank separately into two PRO modules. Comparing these two configurations, DDDF showed worse energy harnessing performance than that of the single, conventional PRO operation. For CDDF, and DDCF, either the draw or the feed was supplied continuously, while the other was treated separately. These two configurations showed better performance than DDDF.

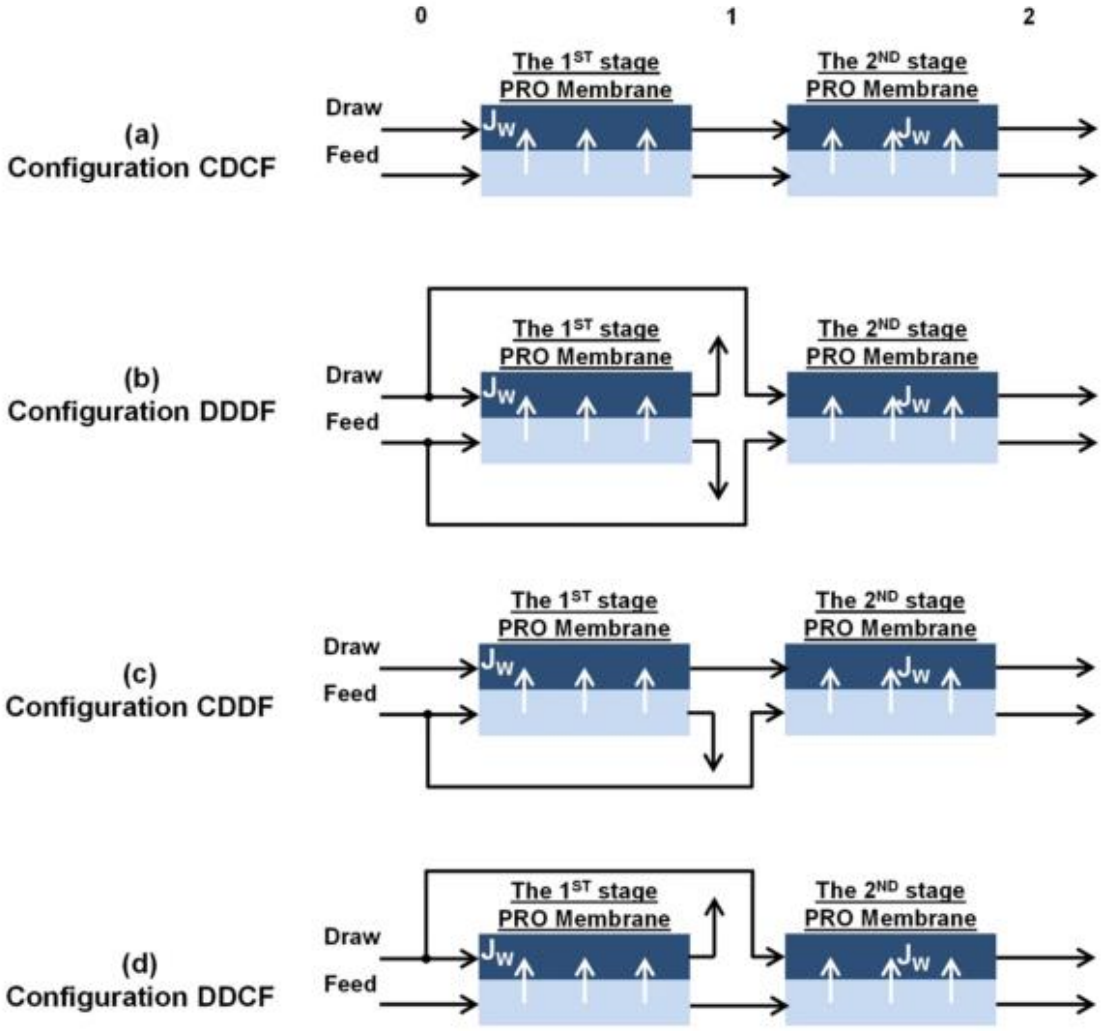


Figure 12. The four different proposed configurations of a dual-stage PRO system: (a) CDCF (continuous draw and feed); (b) DDDF (divided treatment of draw and feed); (c) CDDF (continuous draw and divided feed); and (d) DDCF (divided draw and continuous feed) [191].

### 7.3. Pool PRO

One of the inherent limitations of PRO is its requirement of various mechanical parts, which all require energy to function. One of these mechanical parts is the pressure exchanger, which transfers pressure from the pressurized stream to a non-pressurized stream. Arias and De Las Heras proposed to eliminate the use of the pressure exchanger by the introduction of the pool PRO system, as shown in Figure 13 [192]. In the pool PRO system, the DS is placed in a pool, and the feed was supplied into a stream, until it approaches the semi-permeable membrane, which allows the permeance of fresh water and the buoyancy of the mixed feed and draw will allow the diluted draw to be pulled instantaneously as it is formed. The buoyancy of the diluted draw was expected due to a change in the density of the draw. Due to the pulling away effect of the buoyancy of the diluted draw, the need for the pressure exchanger to pressurize the diluted draw stream was eliminated. No further study was done on pool PRO, but based on the simulations, the pool configuration could prove to be highly beneficial when there is a large amount of DS available.

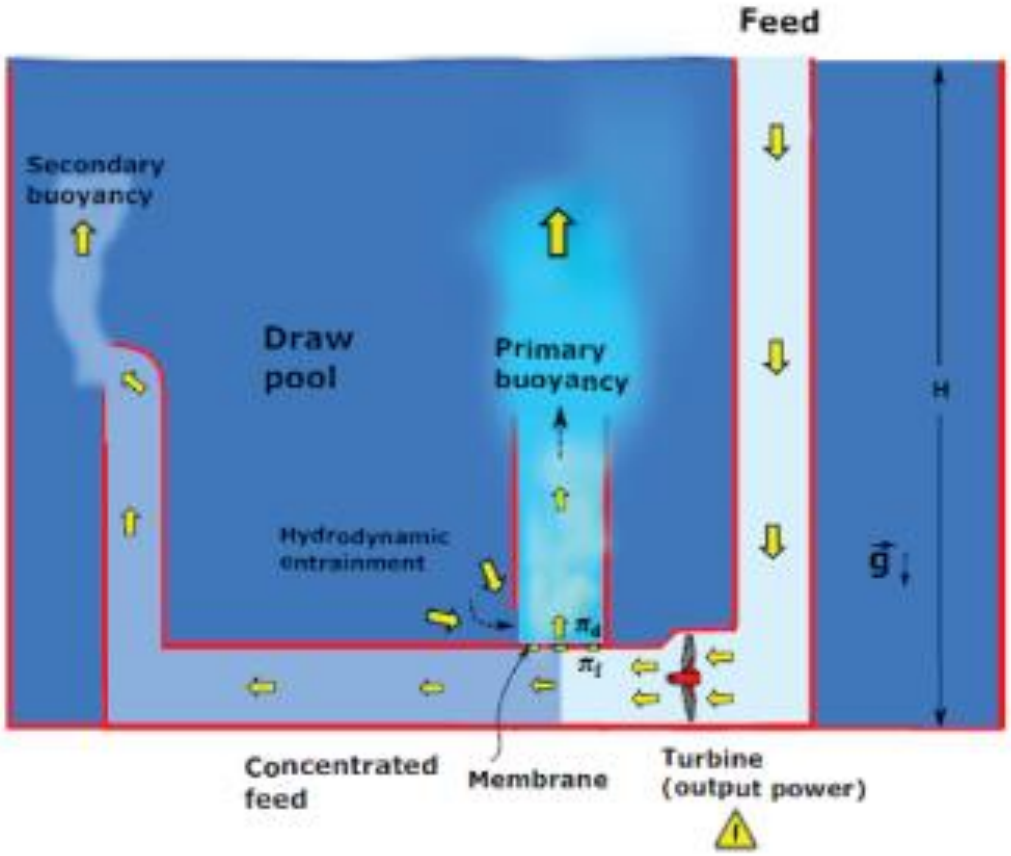


Figure 13. The proposed pool PRO system [192].

7.4. Facultative RO/PRO system

To improve the economic efficiency of a stand-alone PRO system, Blankert et al. [193] proposed a facultative RO and PRO system which does both operations, but not at the same time, as the system switches between the two operating modes, depending on the presence of the DS (Figure 14). The RO mode is activated when only the FS containing wastewater treatment plant effluent is available, resulting in the production of high-quality water. The PRO mode, on the other hand, is activated in the presence of SWRO brine DS, whose salinity difference with the wastewater effluent can be converted into osmotic energy. While this system does not specifically develop PRO as an energy-harnessing process, it is able to provide solutions to improve the process, and find a way to facilitate wastewater treatment along with energy generation.

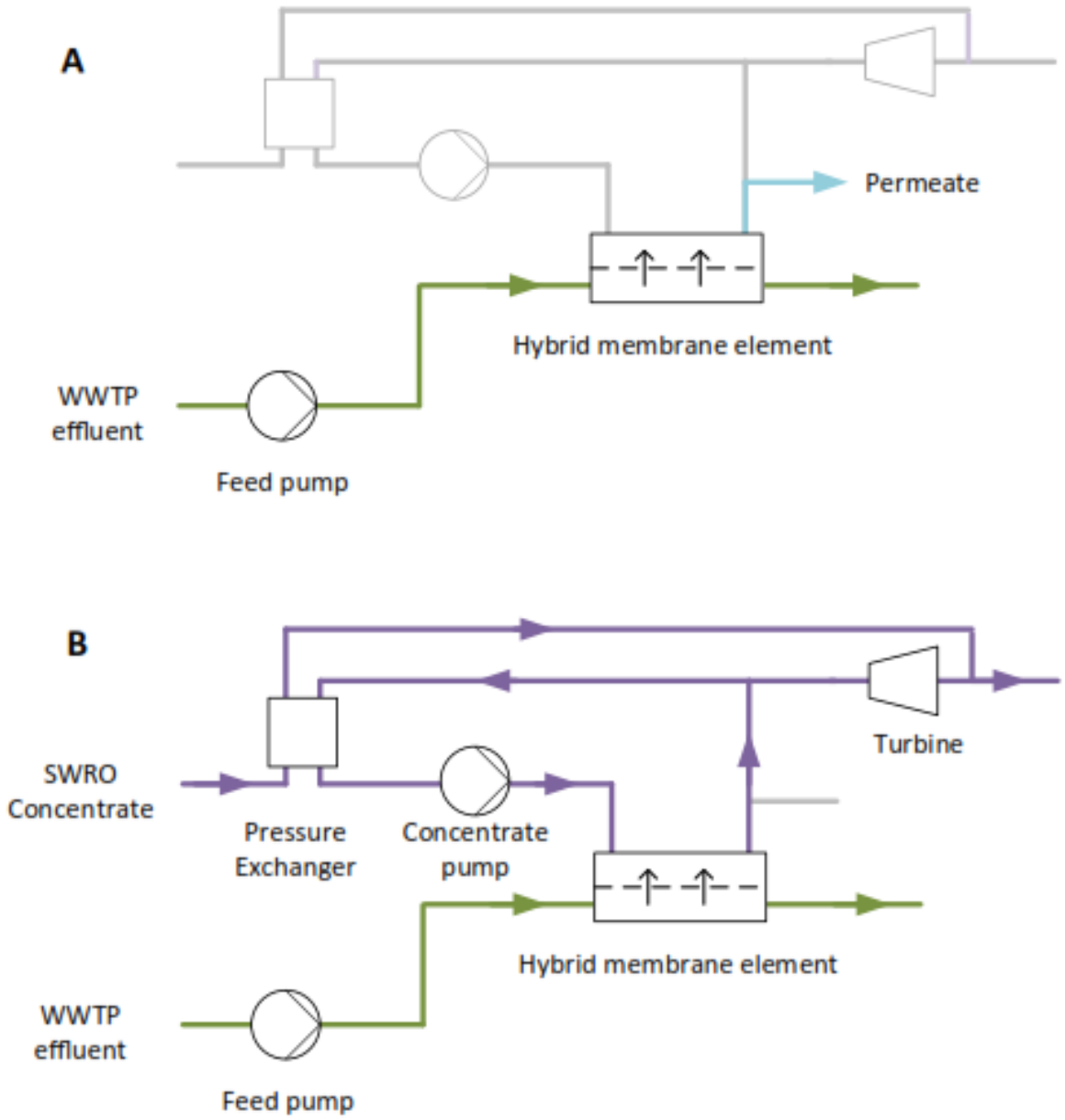


Figure 14. The schematic concept for the proposed facultative RO-PRO system, which can do both (a) RO operation and (b) PRO operation, but not at the same time, as the system switches between the two operating modes [193].

### 7.5. Green PRO

A niche application of PRO was the use of agricultural fertilizers as the draw solute, for a process known as Green PRO [36]. This process was envisioned to be able to generate power, pressurize irrigation water, and treat water, as shown in Figure 15. Pure and mixed agricultural fertilizers were utilized as the draw and

irrigation water (river water) was used as the feed in this study. Theoretical thermodynamic simulation results were validated with experimental data to demonstrate that the dilution of agricultural fertilizers to make these suitable for fertilizer-based irrigation could release chemical potential energy, which could then be harnessed during PRO.

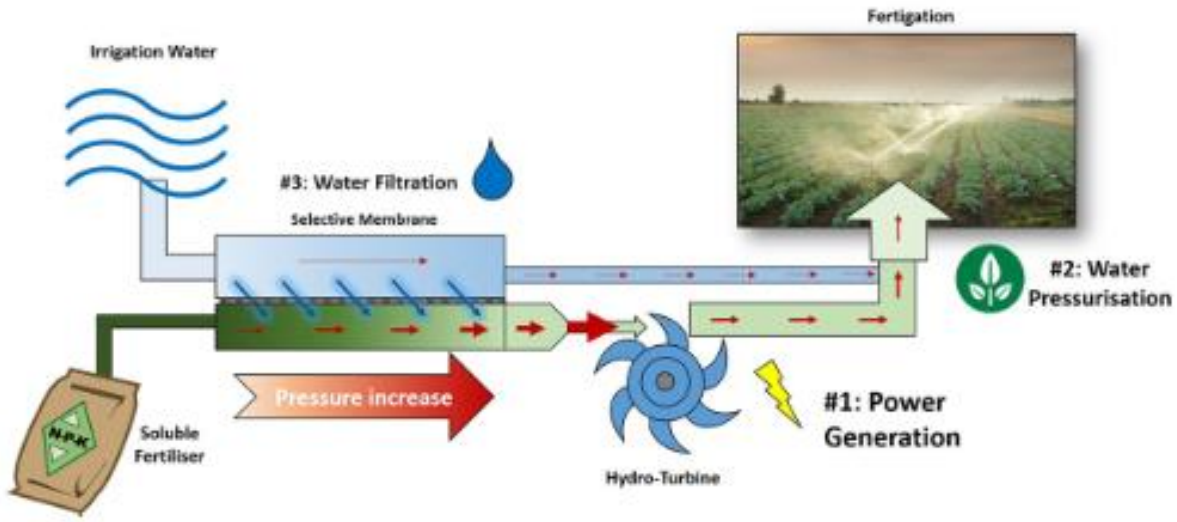


Figure 15. The proposed fertilizer-driven PRO process, Green PRO [36].

7.6. PRO for enhanced oil recovery

A consortium of researchers from Qatar, Australia, and US has an ongoing work on the use of PRO for oil recovery and treatment of produced water from conventional oil sources [194]. The hypersaline nature of produced water from oil sources (amounting to up to 290,000 mg $L^{-1}$ salinity, around 8 times higher than seawater) makes it a suitable DS choice, with seawater or desalination plant brine as the FS. This work is currently ongoing, with a main focus on the following: (1) pretreatment requirements of produced water for PRO DS use, (2) development of suitable membranes which could withstand high pressures required for obtaining peak power densities from the hypersaline produced water, and (3) application of waterflooding with PRO.

Waterflooding is a practice performed in large-scale petroleum industries, wherein the produced water is injected into the oil source to displace the oil, hereby increasing oil production at the wellhead. PRO can be applied alongside waterflooding, as shown in Figure 16. This process is able to reuse the diluted produced water from PRO while simultaneously reducing required pumping energy requirements, reducing waste stream, enhancing injectivity, generate energy, and enhance oil production.

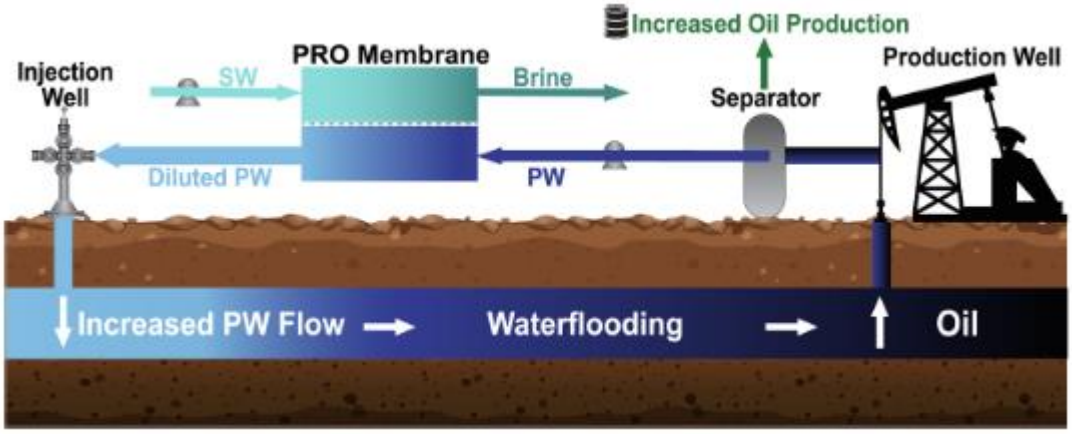


Figure 16. The proposed integrated PRO and waterflooding process, for enhanced oil recovery [195].

### 7.7. Geothermal PRO

A new renewable energy system combining geothermal heat and PRO was recently developed. Named SaltPower, the system uses high salinity geothermal brine in an osmotic power installation coupled with geothermal heat production [196]. As shown in Figure 17, geothermal brine passes through a heat exchanger, in this case, the geothermal heat plant, prior to PRO operation, using various feed sources, such as wastewater. The geothermal heat plant can be used for district heating, while the electricity produced by the PRO operation can be used either for household or geothermal plant use.

Using the geothermal PRO system, single and multi-stage operation designs were investigated. The authors believed that a larger amount of osmotic potential is required to increase salinity gradient production, thus a multi-stage PRO operation could prove useful. Two multi-stage designs were investigated and the

efficiency and performance of these designs were compared with that of the single-stage operation. A single-stage operation was only able to extract 35% of the theoretical extractable salinity gradient energy. One multi-stage PRO design made use of two different membrane modules operated at different pressures, with the draw solution output of the first stage (operated at 50 bar) proceed to both a hydro turbine and the second stage operated at 30 bar. This design resulted to an enhanced salinity gradient energy extraction of 46%. The other multi-stage operation aimed to reduce the loss in the pressure exchanger by using two membranes connected in series, operated at an equal pressure of 50 bar to generate more permeate directed toward the same turbine. The energy extraction capacity improved to over 60% following this approach.

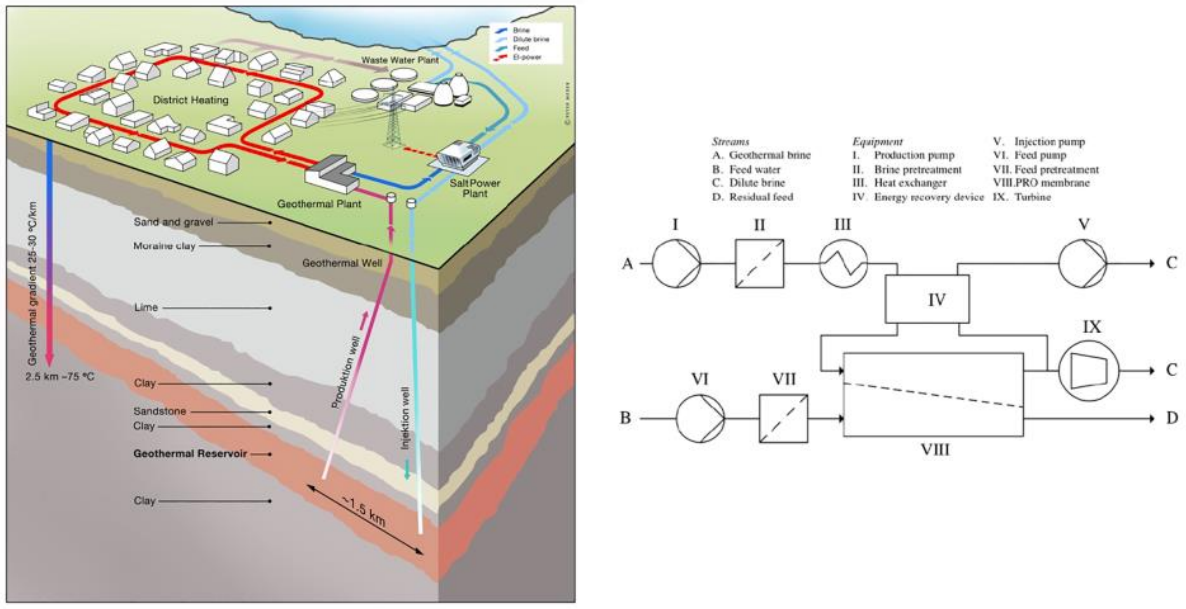


Figure 17. The illustration of the combined PRO and geothermal heat plant system of SaltPower, showing how geothermal heat production and PRO could work together to provide both district heating and electricity. The schematic diagram on the right shows how the geothermal plant acts as the heat exchanger in this system [196].

## 8. Technical challenges, feasibility, and future perspectives

8.1. Technical challenges and feasibility

The current biggest challenge of PRO is the feasibility of the process. PRO researchers have now started to accept that the theoretical energy-harnessing potential of PRO is flawed and there are limitations in the actual demonstration of the process, affecting the maximum thermodynamic energy which can be harnessed from the process, especially when energy expenditures for pretreatment, pressurization, and delivery are to be considered. Straub et al. [22] calculated that the maximum Gibbs free energy extractable from the mixing of seawater (0.6 M NaCl) and river water (0.015 M NaCl) was only 0.26 kWh $m^{-3}$. Taking in consideration the energy requirements for pretreatment (0.1-0.4 kWh $m^{-3}$), pressurization (0.05-0.1 kWh $m^{-3}$), and pumping (0.02-0.05 kWh $m^{-3}$), the amount of net energy will be fractional, that the whole process could be considered futile [15, 150, 197]. However, these energy expenditure assumptions, as well as the cost and economic analysis, do not depict a clear picture of the feasibility of the PRO process, as full-scale PRO power plants are not operated to validate these findings. With the implementation of a full-scale PRO power plant, PRO researchers can also gain insight with the underlying capital, operational, and maintenance costs of the plant.

These information lead to the question of the feasibility and viability of the process. Can the limitations and the underlying costs of PRO operation be offset by the amount of energy harnessed by the process?

Aside from commercialization of the process, large-scale development and commercialization of PRO membranes also remain to be fully achieved. Due to the lack of commercialized membranes for PRO, the unit price of each module is too high, that the total capital cost of PRO operation is also affected. Furthermore, membranes and modules have only a specific lifetime, that during continuous PRO operation of a plant, the replacement, cleaning, and maintenance of the membranes should also be considered. Also, membrane cost may be inversely proportional to membrane durability and efficiency, such that, cheaper membranes may not deliver better performance and longer lifetime, hereby further increasing operational costs [23]. Membrane performance is also highly important in determining the feasibility of the PRO

process. Similarly, membranes with low power density values would require larger membrane size to augment the limited energy harnessing capability of the membrane, thus, increasing capital expenditure. High performance membranes for PRO are expected to be able to decrease energy cost due to the higher energy production of better membranes. If PRO membranes are able to increase power density, membrane life, and minimize energy production cost, then revenues for PRO demonstration would increase.

The recent research direction that PRO is gearing towards is the integrated hybrid processes involving PRO and other applications of PRO. Previous studies have shown that PRO installations as part of a hybrid process are cheaper than a stand-alone PRO power plant, mainly due to the use of already available infrastructure for PRO operation, and the cheaper installation and operational costs of already established and commercial processes, like SWRO and MD [167, 198]. The issues hindering the full-scale implementation and commercialization of PRO has not changed in the past five years. This is the reason why recent research on process development for PRO has gone from pilot-scale applications to development of hybrid PRO processes and finding niche applications for PRO. Development of hybrid PRO processes and niche applications for PRO could then use the extractable energy of PRO to augment energy requirements of other processes or find suitable applications for PRO, which would not require expensive infrastructure construction or intensive energy consumption due to pumping and pressurization.

### 8.2. Future perspectives

The PRO process is a promising technology to harness renewable power from natural salinity gradient. Through utilizing a suitable membrane to control the spontaneous mixing of the saline solutions, the salinity gradient energy can be extracted in terms of electricity using the PRO system with reduced environmental impacts. The concept of this PRO process has been reported in the last decade, however, due to failure in both sustainable large-scale PRO implementation and development of suitable membranes and modules, PRO research has not significantly advanced as many researchers had hoped. Different PRO

configurations, as well as multi-stage or hybridized process designs, have been recently investigated to improve the overall process efficiency while minimizing energy requirements and operational cost. Also recently, bench-scale membrane development studies have achieved outstanding PRO performance with membranes prepared by a variety of techniques, which include chemical modification and material incorporation. While these membranes were able to achieve excellent bench-scale performance, the real challenge is cost-effective and consistent fabrication of such membranes at a larger scale, potentially for modulation. In literature, nano-sized material incorporation and chemical modification have become popular membrane development research trends to alter the properties and separation performance of the membrane; however, the material synthesis cost and the process optimization for effective and consistent incorporation and modification are some of these technique's limitations. Furthermore, module development is the next necessary step. High-performance membranes are required for PRO; however, membrane modulation was found to be more important in a sustainable PRO process operation [150]. Membrane modules should be designed such that pressure drop is limited, the membrane weak points are minimized, and the membranes do not sustain damage over constant operation at a higher pressure [199].

New emerging trends involve advanced configurations and niche applications of the PRO process. Due to these processes, salinity gradient energy can be harnessed using a wide variety of draw and feed solutions. Not only that, integrated processes are able to perform more than just salinity gradient energy generation, but also seawater desalination, wastewater treatment, heat recovery, and valuable resource recovery. These technologies can effectively be utilized for maximizing the power density with excellent heat recovery and energy efficiency when coupled with other membrane desalination technology. The dual-stage closed loop PRO process is a potential method that can achieve more efficient performance than the single-stage PRO process due to high water permeation in the second stage. Furthermore, future PRO studies should also focus on the further development of hybrid processes and large-scale installation of pilot plants. Following the efforts of the Mega-ton and GMVP projects in Japan and South Korea, respectively, it was found that

SWRO-PRO demonstration plant can achieve maximum power density of about 18.3 W $m^{-2}$ and the energy consumption can be decreased by 80% when desalinating 240 $m^3$ $d^{-1}$ of seawater.

It is also believed that the pretreatment strategies can reduce PRO membrane fouling, decrease the need for chemical cleaning and module replacement, and increase the membrane life time. The RO-NF-PRO hybrid process is an outstanding system, which integrates these membrane processes to simultaneously attain three objectives: (1) pre-concentration of DS for higher extractable salinity gradient energy, (2) pretreatment of the feed, and (3) salinity gradient energy harnessing. Other pretreatment conditions can also be considered, depending on the nature of the FS and DS.

Despite the difficulty in proving the feasibility of PRO as a commercially viable process, this process still has a huge commercial potential. The failure of Statkraft and the lack of follow-up after the high-profile Mega-ton and GMVP SWRO-PRO pilot plant projects prove to be discouraging; however, these projects were able to provide significant insights regarding the implementation of PRO. Based on these pilot-scale implementations, the stand-alone PRO process has proven difficult to be implemented, and would require a more systemic process design and optimization to address the inherent limitations of the process, as well as more careful evaluation of economic potential. On the other hand, integration with other membrane-based processes has shown promising results, and with better configurations and operating conditions, the GMVP project will definitely not be the last full-scale implementation for PRO, as many membrane engineers and researchers are finding ways to exploit this process and improve its efficiency. In fact, the Middle East is starting to look at PRO to augment the diminishing fresh water supply in the region, while generating salinity gradient energy. Also, SaltPower has recently shown the feasibility of its geothermal PRO system installation in simultaneous district heating and energy generation. With continuous effort in development of PRO processes, membranes, and modules, the economically feasible extractable power density requirement of 5 W $m^{-2}$, originally set by Statkraft, could be achieved in the future.

**Acknowledgment**

This research is supported by a grant from the Qatar National Research Fund under its National Priorities Research Program (Award Number NPRP 10-1231-160069).

**References:**

[1] T.-S. Chung, X. Li, R.C. Ong, Q. Ge, H. Wang, G. Han, Emerging forward osmosis (FO) technologies and challenges ahead for clean water and clean energy applications, Current Opinion in Chemical Engineering, 1 (2012) 246-257.

[2] R.R. Gonzales, S.-H. Kim, Dark fermentative hydrogen production following the sequential dilute acid pretreatment and enzymatic saccharification of rice husk, International Journal of Hydrogen Energy, 42 (2017) 27577-27583.

[3] S. Shafiee, E. Topal, When will fossil fuel reserves be diminished?, Energy Policy, 37 (2009) 181-189.

[4] B. Kruyt, D.P. van Vuuren, H.J.M. de Vries, H. Groenenberg, Indicators for energy security, Energy Policy, 37 (2009) 2166-2181.

[5] T.L. Root, J.T. Price, K.R. Hall, S.H. Schneider, C. Rosenzweig, J.A. Pounds, Fingerprints of global warming on wild animals and plants, Nature, 421 (2003) 57-60.

[6] S.A. Kalogirou, Seawater desalination using renewable energy sources, Progress in Energy and Combustion Science, 31 (2005) 242-281.

[7] K. Touati, F. Tadeo, Green energy generation by pressure retarded osmosis: State of the art and technical advancement—review, International Journal of Green Energy, 14 (2017) 337-360.

[8] R.R. Gonzales, J.S. Kim, S.-H. Kim, Optimization of dilute acid and enzymatic hydrolysis for dark fermentative hydrogen production from the empty fruit bunch of oil palm, International Journal of Hydrogen Energy, 44 (2019) 2191-2202.

[9] R.R. Gonzales, G. Kumar, P. Sivagurunathan, S.-H. Kim, Enhancement of hydrogen production by optimization of pH adjustment and separation conditions following dilute acid pretreatment of lignocellulosic biomass, International Journal of Hydrogen Energy, 42 (2017) 27502-27511.

[10] S. Sgouridis, D. Csala, A Framework for Defining Sustainable Energy Transitions: Principles, Dynamics, and Implications, Sustainability, 6 (2014).

[11] H. Kim, J.S. Choi, S. Lee, Pressure retarded osmosis for energy production: Membrane materials and operating conditions, Water Science and Technology, 65 (2012) 1789-1794.

[12] J.W. Post, J. Veerman, H.V.M. Hamelers, G.J.W. Euverink, S.J. Metz, K. Nymeijer, C.J.N. Buisman, Salinity-gradient power: Evaluation of pressure-retarded osmosis and reverse electrodialysis, Journal of Membrane Science, 288 (2007) 218-230.

[13] O. Alvarez-Silva, A.F. Osorio, Salinity gradient energy potential in Colombia considering site specific constraints, Renewable Energy, 74 (2015) 737-748.

[14] O.S. Burheim, F. Liu, B.B. Sales, O. Schaetzle, C.J.N. Buisman, H.V.M. Hamelers, Faster Time Response by the Use of Wire Electrodes in Capacitive Salinity Gradient Energy Systems, The Journal of Physical Chemistry C, 116 (2012) 19203-19210.

[15] S. Lin, A.P. Straub, M. Elimelech, Thermodynamic limits of extractable energy by pressure retarded osmosis, Energy & Environmental Science, 7 (2014) 2706-2714.

[16] B. Nicolaisen, Developments in membrane technology for water treatment, Desalination, 153 (2003) 355-360.
[17] D.I. Kim, R.R. Gonzales, P. Dorji, G. Gwak, S. Phuntsho, S. Hong, H. Shon, Efficient recovery of nitrate from municipal wastewater via MCDI using anion-exchange polymer coated electrode embedded with nitrate selective resin, Desalination, 484 (2020) 114425.
[18] W. Guo, H.-H. Ngo, J. Li, A mini-review on membrane fouling, Bioresource Technology, 122 (2012) 27-34.
[19] H. Strathmann, Membrane separation processes: Current relevance and future opportunities, AIChE Journal, 47 (2001) 1077-1087.
[20] M. Elimelech, W.A. Phillip, The future of seawater desalination: Energy, technology, and the environment, Science, 333 (2011) 712.
[21] N.Y. Yip, M. Elimelech, Comparison of energy efficiency and power density in pressure retarded osmosis and reverse electrodialysis, Environmental Science & Technology, 48 (2014) 11002-11012.
[22] A.P. Straub, A. Deshmukh, M. Elimelech, Pressure-retarded osmosis for power generation from salinity gradients: is it viable?, Energy & Environmental Science, 9 (2016) 31-48.
[23] A. Achilli, A.E. Childress, Pressure retarded osmosis: From the vision of Sidney Loeb to the first prototype installation - Review, Desalination, 261 (2010) 205-211.
[24] F. Helfer, C. Lemckert, Y.G. Anissimov, Osmotic power with pressure retarded osmosis: Theory, performance and trends – A review, Journal of Membrane Science, 453 (2014) 337-358.
[25] N.H. D. Johnson, Characterisation and quantification of membrane surface properties using atomic force microscopy: A comprehensive review, Desalination, 356 (2015) 149–164.
[26] Y. Chun, D. Mulcahy, L. Zou, I.S. Kim, A short review of membrane fouling in forward osmosis processes, Membranes, 7 (2017) 30.
[27] J.K. D. I. Kim, H. K. Shon, S. Hong, Pressure retarded osmosis (PRO) for integrating seawater desalination and wastewater reclamation: Energy consumption and fouling, Journal of Membrane Science 483 (2015) 34–41.
[28] E. Nagy, I. Hegedüs, E.W. Tow, J.H. Lienhard V, Effect of fouling on performance of pressure retarded osmosis (PRO) and forward osmosis (FO), Journal of Membrane Science, 565 (2018) 450-462.
[29] Z.L. K. Yang, H. Zhang, J. Qian, G. Chen, Municipal wastewater phosphorus removal by coagulation, J. Environ. Sci., 31 (2010) 601–609.
[30] T.-S. Chung, L. Luo, C.F. Wan, Y. Cui, G. Amy, What is next for forward osmosis (FO) and pressure retarded osmosis (PRO), Separation and Purification Technology, 156 (2015) 856-860.
[31] K. Gerstandt, K.V. Peinemann, S.E. Skilhagen, T. Thorsen, T. Holt, Membrane processes in energy supply for an osmotic power plant, Desalination, 224 (2008) 64-70.
[32] B.E. Logan, M. Elimelech, Membrane-based processes for sustainable power generation using water, Nature, 488 (2012) 313.
[33] S. Loeb, G.D. Mehta, A two-coefficient water transport equation for pressure-retarded osmosis, Journal of Membrane Science, 4 (1978) 351-362.

[34] S. Loeb, Production of energy from concentrated brines by pressure-retarded osmosis: I. Preliminary technical and economic correlations, Journal of Membrane Science, 1 (1976) 49-63.
[35] N.Y. Yip, A. Tiraferri, W.A. Phillip, J.D. Schiffman, L.A. Hoover, Y.C. Kim, M. Elimelech, Thin-film composite pressure retarded osmosis membranes for sustainable power generation from salinity gradients, Environmental Science & Technology, 45 (2011) 4360-4369.
[36] F. Volpin, R.R. Gonzales, S. Lim, N. Pathak, S. Phuntsho, H.K. Shon, GreenPRO: A novel fertiliser-driven osmotic power generation process for fertigation, Desalination, 447 (2018) 158-166.
[37] A.F.I. N. Hilal, M. Kh. Souhaimi, D. Johnson, Osmosis engineering, Elsevier, Oxford, 2020.
[38] Y.C. Kim, M. Elimelech, Potential of osmotic power generation by pressure retarded osmosis using seawater as feed solution: Analysis and experiments, Journal of Membrane Science, 429 (2013) 330-337.
[39] S.E. Skilhagen, J.E. Dugstad, R.J. Aaberg, Osmotic power — power production based on the osmotic pressure difference between waters with varying salt gradients, Desalination, 220 (2008) 476-482.
[40] T.Y. Cath, A.E. Childress, M. Elimelech, Forward osmosis: Principles, applications, and recent developments, Journal of Membrane Science, 281 (2006) 70-87.
[41] Z.L. S. Sarp, J. Saththasivam, Pressure Retarded Osmosis (PRO): Past experiences, current developments, and future prospects, Desalination 389 (2016) 2–14.
[42] W.A.S. D. J. Johnson, A. Mohammed, N. Hilal,, Osmotic's potential: An overview of draw solutes for forward osmosis, Desalination, 434 (2018) 100–120.
[43] R.R. Gonzales, M.J. Park, L. Tijing, D.S. Han, S. Phuntsho, H.K. Shon, Modification of nanofiber support layer for thin film composite forward osmosis membranes via layer-by-layer polyelectrolyte deposition, Membranes, 8 (2018) 70-84.
[44] K.L. Lee, R.W. Baker, H.K. Lonsdale, Membranes for power generation by pressure-retarded osmosis, Journal of Membrane Science, 8 (1981) 141-171.
[45] A. Achilli, T.Y. Cath, A.E. Childress, Power generation with pressure retarded osmosis: An experimental and theoretical investigation, Journal of Membrane Science, 343 (2009) 42-52.
[46] A. Tiraferri, N.Y. Yip, W.A. Phillip, J.D. Schiffman, M. Elimelech, Relating performance of thin-film composite forward osmosis membranes to support layer formation and structure, Journal of Membrane Science, 367 (2011) 340-352.
[47] C.H. Tan, H.Y. Ng, Revised external and internal concentration polarization models to improve flux prediction in forward osmosis process, Desalination, 309 (2013) 125-140.
[48] K. Touati, F. Tadeo, Study of the reverse salt diffusion in pressure retarded osmosis: Influence on concentration polarization and effect of the operating conditions, Desalination, 389 (2016) 171-186.
[49] J.R. McCutcheon, M. Elimelech, Influence of concentrative and dilutive internal concentration polarization on flux behavior in forward osmosis, Journal of Membrane Science, 284 (2006) 237-247.
[50] Z. Zhou, J.Y. Lee, T.-S. Chung, Thin film composite forward-osmosis membranes with enhanced internal osmotic pressure for internal concentration polarization reduction, Chemical Engineering Journal, 249 (2014) 236-245.
[51] J.R. McCutcheon, M. Elimelech, Influence of membrane support layer hydrophobicity on water flux

in osmotically driven membrane processes, Journal of Membrane Science, 318 (2008) 458-466.
[52] E.W. Tow, R.K. McGovern, J.H. Lienhard V, Raising forward osmosis brine concentration efficiency through flow rate optimization, Desalination, 366 (2015) 71-79.
[53] D.J.J. W. A. Suwaileh, S. Sarp, N. Hilal, Advances in forward osmosis membranes: Altering the sub-layer structure via recent fabrication and chemical modification approaches, Desalination 436 (2018) 176–201.
[54] J.Z. A. Altaee, A. A. Alanezi, G. Zaragoza, Pressure retarded osmosis process for power generation: Feasibility, energy balance and controlling parameters, Applied Energy, 206 (2017) 303–311.
[55] N.Y. Yip, M. Elimelech, Influence of natural organic matter fouling and osmotic backwash on pressure retarded osmosis energy production from natural salinity gradients, Environmental Science & Technology, 47 (2013) 12607-12616.
[56] W.R. Thelin, E. Sivertsen, T. Holt, G. Brekke, Natural organic matter fouling in pressure retarded osmosis, Journal of Membrane Science, 438 (2013) 46-56.
[57] Q. She, Y.K.W. Wong, S. Zhao, C.Y. Tang, Organic fouling in pressure retarded osmosis: Experiments, mechanisms and implications, Journal of Membrane Science, 428 (2013) 181-189.
[58] M. Zhang, D. Hou, Q. She, C.Y. Tang, Gypsum scaling in pressure retarded osmosis: Experiments, mechanisms and implications, Water Research, 48 (2014) 387-395.
[59] J. Kim, M.J. Park, M. Park, H.K. Shon, S.-H. Kim, J.H. Kim, Influence of colloidal fouling on pressure retarded osmosis, Desalination, 389 (2016) 207-214.
[60] S.C. Chen, C.F. Wan, T.-S. Chung, Enhanced fouling by inorganic and organic foulants on pressure retarded osmosis (PRO) hollow fiber membranes under high pressures, Journal of Membrane Science, 479 (2015) 190-203.
[61] Q. She, L. Zhang, R. Wang, W.B. Krantz, A.G. Fane, Pressure-retarded osmosis with wastewater concentrate feed: Fouling process considerations, Journal of Membrane Science, 542 (2017) 233-244.
[62] S.C. Chen, G.L. Amy, T.-S. Chung, Membrane fouling and anti-fouling strategies using RO retentate from a municipal water recycling plant as the feed for osmotic power generation, Water Research, 88 (2016) 144-155.
[63] E. Bar-Zeev, F. Perreault, A.P. Straub, M. Elimelech, Impaired performance of pressure-retarded osmosis due to irreversible biofouling, Environmental Science & Technology, 49 (2015) 13050-13058.
[64] E. Abbasi-Garravand, C.N. Mulligan, C.B. Laflamme, G. Clairet, Role of two different pretreatment methods in osmotic power (salinity gradient energy) generation, Renewable Energy, 96 (2016) 98-119.
[65] T. Yang, C.F. Wan, J.Y. Xiong, T.-S. Chung, Pre-treatment of wastewater retentate to mitigate fouling on the pressure retarded osmosis (PRO) process, Separation and Purification Technology, 215 (2019) 390-397.
[66] Y. Chen, C. Liu, L. Setiawan, Y.-N. Wang, X. Hu, R. Wang, Enhancing pressure retarded osmosis performance with low-pressure nanofiltration pretreatment: Membrane fouling analysis and mitigation, Journal of Membrane Science, 543 (2017) 114-122.
[67] C.F. Wan, S. Jin, T.-S. Chung, Mitigation of inorganic fouling on pressure retarded osmosis (PRO)

membranes by coagulation pretreatment of the wastewater concentrate feed, Journal of Membrane Science, 572 (2019) 658-667.
[68] G. Han, J. Zhou, C. Wan, T. Yang, T.-S. Chung, Investigations of inorganic and organic fouling behaviors, antifouling and cleaning strategies for pressure retarded osmosis (PRO) membrane using seawater desalination brine and wastewater, Water Research, 103 (2016) 264-275.
[69] D.I. Kim, J. Kim, S. Hong, Changing membrane orientation in pressure retarded osmosis for sustainable power generation with low fouling, Desalination, 389 (2016) 197-206.
[70] X. Li, T. Cai, G.L. Amy, T.-S. Chung, Cleaning strategies and membrane flux recovery on anti-fouling membranes for pressure retarded osmosis, Journal of Membrane Science, 522 (2017) 116-123.
[71] E.S.H. Lee, J.Y. Xiong, G. Han, C.F. Wan, Q.Y. Chong, T.-S. Chung, A pilot study on pressure retarded osmosis operation and effective cleaning strategies, Desalination, 420 (2017) 273-282.
[72] S.C. Chen, X.Z. Fu, T.-S. Chung, Fouling behaviors of polybenzimidazole (PBI)–polyhedral oligomeric silsesquioxane (POSS)/polyacrylonitrile (PAN) hollow fiber membranes for engineering osmosis processes, Desalination, 335 (2014) 17-26.
[73] S. Zhang, Y. Zhang, T.-S. Chung, Facile preparation of antifouling hollow fiber membranes for sustainable osmotic power generation, ACS Sustainable Chemistry & Engineering, 4 (2016) 1154-1160.
[74] Y. Li, S. Qi, Y. Wang, L. Setiawan, R. Wang, Modification of thin film composite hollow fiber membranes for osmotic energy generation with low organic fouling tendency, Desalination, 424 (2017) 131-139.
[75] D. Zhao, G. Qiu, X. Li, C. Wan, K. Lu, T.-S. Chung, Zwitterions coated hollow fiber membranes with enhanced antifouling properties for osmotic power generation from municipal wastewater, Water Research, 104 (2016) 389-396.
[76] G. Han, J.T. Liu, K.J. Lu, T.-S. Chung, Advanced anti-fouling membranes for osmotic power generation from wastewater via pressure retarded osmosis (PRO), Environmental Science & Technology, 52 (2018) 6686-6694.
[77] T. Cai, X. Li, C. Wan, T.-S. Chung, Zwitterionic polymers grafted poly (ether sulfone) hollow fiber membranes and their antifouling behaviors for osmotic power generation, Journal of Membrane Science, 497 (2016) 142-152.
[78] L. Zhang, Q. She, R. Wang, S. Wongchitphimon, Y. Chen, A.G. Fane, Unique roles of aminosilane in developing anti-fouling thin film composite (TFC) membranes for pressure retarded osmosis (PRO), Desalination, 389 (2016) 119-128.
[79] Y. Zhang, J.L. Li, T. Cai, Z.L. Cheng, X. Li, T.-S. Chung, Sulfonated hyperbranched polyglycerol grafted membranes with antifouling properties for sustainable osmotic power generation using municipal wastewater, Journal of Membrane Science, 563 (2018) 521-530.
[80] X. Li, T. Cai, T.-S. Chung, Anti-fouling behavior of hyperbranched polyglycerol-grafted poly(ether sulfone) hollow fiber membranes for osmotic power generation, Environmental Science & Technology, 48 (2014) 9898-9907.
[81] J.L. Li, Y. Zhang, S. Zhang, M. Liu, X. Li, T. Cai, Hyperbranched poly(ionic liquid) functionalized

poly(ether sulfone) membranes as healable antifouling coatings for osmotic power generation, Journal of Materials Chemistry A, 7 (2019) 8167-8176.
[82] D.L. Zhao, S. Das, T.-S. Chung, Carbon quantum dots grafted antifouling membranes for osmotic power generation via pressure-retarded osmosis process, Environmental Science & Technology, 51 (2017) 14016-14023.
[83] Y. Kim, E. Yang, H. Park, H. Choi, Anti-biofouling effect of a thin film nanocomposite membrane with a functionalized-carbon-nanotube-blended polymeric support for the pressure-retarded osmosis process, RSC Advances, 10 (2020) 5697-5703.
[84] J. Kim, D. Suh, C. Kim, Y. Baek, B. Lee, H.J. Kim, J.-C. Lee, J. Yoon, A high-performance and fouling resistant thin-film composite membrane prepared via coating TiO2 nanoparticles by sol-gel-derived spray method for PRO applications, Desalination, 397 (2016) 157-164.
[85] S. Lim, M.J. Park, S. Phuntsho, A. Mai-Prochnow, A.B. Murphy, D. Seo, H. Shon, Dual-layered nanocomposite membrane incorporating graphene oxide and halloysite nanotube for high osmotic power density and fouling resistance, Journal of Membrane Science, 564 (2018) 382-393.
[86] X. Liu, L.-X. Foo, Y. Li, J.-Y. Lee, B. Cao, C.Y. Tang, Fabrication and characterization of nanocomposite pressure retarded osmosis (PRO) membranes with excellent anti-biofouling property and enhanced water permeability, Desalination, 389 (2016) 137-148.
[87] G. Han, Z.L. Cheng, T.-S. Chung, Thin-film composite (TFC) hollow fiber membrane with double-polyamide active layers for internal concentration polarization and fouling mitigation in osmotic processes, Journal of Membrane Science, 523 (2017) 497-504.
[88] Q. She, X. Jin, C.Y. Tang, Osmotic power production from salinity gradient resource by pressure retarded osmosis: Effects of operating conditions and reverse solute diffusion, Journal of Membrane Science, 401 (2012) 262-273.
[89] S. Loeb, F. Van Hessen, D. Shahaf, Production of energy from concentrated brines by pressure-retarded osmosis: II. Experimental results and projected energy costs, Journal of Membrane Science, 1 (1976) 249-269.
[90] G.D. Mehta, S. Loeb, Performance of permasep B-9 and B-10 membranes in various osmotic regions and at high osmotic pressures, Journal of Membrane Science, 4 (1979) 335-349.
[91] G.D. Mehta, S. Loeb, Internal polarization in the porous substructure of a semipermeable membrane under pressure-retarded osmosis, Journal of Membrane Science, 4 (1978) 261-265.
[92] S. Loeb, The Loeb-Sourirajan Membrane: How It Came About, in: Synthetic Membranes:, AMERICAN CHEMICAL SOCIETY, 1981, pp. 1-9.
[93] T. Thorsen, T. Holt, The potential for power production from salinity gradients by pressure retarded osmosis, Journal of Membrane Science, 335 (2009) 103-110.
[94] A.F.I. N. Hilal, Ch. Wright, Membrane fabrication, CRC Press, London, 2015.
[95] I. Alsvik, M.-B. Hägg, Pressure retarded osmosis and forward osmosis membranes: Materials and methods, Polymers, 5 (2013) 303.
[96] S. Chou, L. Shi, R. Wang, C.Y. Tang, C. Qiu, A.G. Fane, Characteristics and potential applications

of a novel forward osmosis hollow fiber membrane, Desalination, 261 (2010) 365-372.
[97] Y. Li, R. Wang, S. Qi, C.Y. Tang, Structural stability and mass transfer properties of pressure retarded osmosis (PRO) membrane under high operating pressures, Journal of Membrane Science, 488 (2015) 142-153.
[98] G. Han, S. Zhang, X. Li, T.-S. Chung, High performance thin film composite pressure retarded osmosis (PRO) membranes for renewable salinity-gradient energy generation, Journal of Membrane Science, 440 (2013) 108-121.
[99] Y. Cui, X.-Y. Liu, T.-S. Chung, Enhanced osmotic energy generation from salinity gradients by modifying thin film composite membranes, Chemical Engineering Journal, 242 (2014) 195-203.
[100] X. Li, S. Zhang, F. Fu, T.-S. Chung, Deformation and reinforcement of thin-film composite (TFC) polyamide-imide (PAI) membranes for osmotic power generation, Journal of Membrane Science, 434 (2013) 204-217.
[101] Q. She, J. Wei, N. Ma, V. Sim, A.G. Fane, R. Wang, C.Y. Tang, Fabrication and characterization of fabric-reinforced pressure retarded osmosis membranes for osmotic power harvesting, Journal of Membrane Science, 504 (2016) 75-88.
[102] J.A. Idarraga-Mora, D.A. Ladner, S.M. Husson, Thin-film composite membranes on polyester woven mesh with variable opening size for pressure-retarded osmosis, Journal of Membrane Science, 549 (2018) 251-259.
[103] Y. Sun, L. Cheng, T. Shintani, Y. Tanaka, T. Takahashi, T. Itai, S. Wang, L. Fang, H. Matsuyama, Development of high-flux and robust reinforced aliphatic polyketone thin-film composite membranes for osmotic power generation: Role of reinforcing materials, Industrial & Engineering Chemistry Research, 57 (2018) 13528-13538.
[104] M.K. N. Hilal, Ch. J. Wright, Membrane modification: Technology and applications, CRC Press, London, 2012.
[105] S. Zhang, F. Fu, T.-S. Chung, Substrate modifications and alcohol treatment on thin film composite membranes for osmotic power, Chemical Engineering Science, 87 (2013) 40-50.
[106] M. Son, H. Park, L. Liu, H. Choi, J.H. Kim, H. Choi, Thin-film nanocomposite membrane with CNT positioning in support layer for energy harvesting from saline water, Chemical Engineering Journal, 284 (2016) 68-77.
[107] R.R. Gonzales, M.J. Park, T.-H. Bae, Y. Yang, A. Abdel-Wahab, S. Phuntsho, H.K. Shon, Melamine-based covalent organic framework-incorporated thin film nanocomposite membrane for enhanced osmotic power generation, Desalination, 459 (2019) 10-19.
[108] S.J. Kwon, K. Park, D.Y. Kim, M. Zhan, S. Hong, J.-H. Lee, High-performance and durable pressure retarded osmosis membranes fabricated using hydrophilized polyethylene separators, Journal of Membrane Science, 619 (2021) 118796.
[109] J. Wei, Y. Li, L. Setiawan, R. Wang, Influence of macromolecular additive on reinforced flat-sheet thin film composite pressure-retarded osmosis membranes, Journal of Membrane Science, 511 (2016) 54-64.

[110] S.W. Kim, S.O. Han, I.N. Sim, J.Y. Cheon, W.H. Park, Fabrication and characterization of cellulose acetate/montmorillonite composite nanofibers by electrospinning, Journal of Nanomaterials, 2015 (2015) 1-8.
[111] X. Song, Z. Liu, D.D. Sun, Energy recovery from concentrated seawater brine by thin-film nanofiber composite pressure retarded osmosis membranes with high power density, Energy & Environmental Science, 6 (2013) 1199-1210.
[112] N.-N. Bui, J.R. McCutcheon, Nanofiber supported thin-film composite membrane for pressure-retarded osmosis, Environmental Science & Technology, 48 (2014) 4129-4136.
[113] M. Tian, R. Wang, K. Goh, Y. Liao, A.G. Fane, Synthesis and characterization of high-performance novel thin film nanocomposite PRO membranes with tiered nanofiber support reinforced by functionalized carbon nanotubes, Journal of Membrane Science, 486 (2015) 151-160.
[114] J.H. Kim, S.J. Moon, S.H. Park, M. Cook, A.G. Livingston, Y.M. Lee, A robust thin film composite membrane incorporating thermally rearranged polymer support for organic solvent nanofiltration and pressure retarded osmosis, Journal of Membrane Science, 550 (2018) 322-331.
[115] S.J. Moon, J.H. Kim, J.G. Seong, W.H. Lee, S.H. Park, S.H. Noh, J.H. Kim, Y.M. Lee, Thin film composite on fluorinated thermally rearranged polymer nanofibrous membrane achieves power density of 87 W m−2 in pressure retarded osmosis, improving economics of osmotic heat engine, Journal of Membrane Science, 607 (2020) 118120.
[116] S.J. Moon, S.M. Lee, J.H. Kim, S.H. Park, H.H. Wang, J.H. Kim, Y.M. Lee, A highly robust and water permeable thin film composite membranes for pressure retarded osmosis generating 26 W·m−2 at 21 bar, Desalination, 483 (2020) 114409.
[117] N.-N. Bui, M.L. Lind, E.M.V. Hoek, J.R. McCutcheon, Electrospun nanofiber supported thin film composite membranes for engineered osmosis, Journal of Membrane Science, 385-386 (2011) 10-19.
[118] N. Peng, N. Widjojo, P. Sukitpaneenit, M.M. Teoh, G.G. Lipscomb, T.-S. Chung, J.-Y. Lai, Evolution of polymeric hollow fibers as sustainable technologies: Past, present, and future, Progress in Polymer Science, 37 (2012) 1401-1424.
[119] E. Sivertsen, T. Holt, W. Thelin, G. Brekke, Modelling mass transport in hollow fibre membranes used for pressure retarded osmosis, Journal of Membrane Science, 417-418 (2012) 69-79.
[120] E. Sivertsen, T. Holt, W. Thelin, G. Brekke, Pressure retarded osmosis efficiency for different hollow fibre membrane module flow configurations, Desalination, 312 (2013) 107-123.
[121] G. Han, S. Zhang, X. Li, T.-S. Chung, Progress in pressure retarded osmosis (PRO) membranes for osmotic power generation, Progress in Polymer Science, 51 (2015) 1-27.
[122] S. Chou, R. Wang, L. Shi, Q. She, C. Tang, A.G. Fane, Thin-film composite hollow fiber membranes for pressure retarded osmosis (PRO) process with high power density, Journal of Membrane Science, 389 (2012) 25-33.
[123] S. Chou, R. Wang, A.G. Fane, Robust and high performance hollow fiber membranes for energy harvesting from salinity gradients by pressure retarded osmosis, Journal of Membrane Science, 448 (2013) 44-54.

[124] S. Zhang, P. Sukitpaneenit, T.-S. Chung, Design of robust hollow fiber membranes with high power density for osmotic energy production, Chemical Engineering Journal, 241 (2014) 457-465.
[125] W. Gai, X. Li, J.Y. Xiong, C.F. Wan, T.-S. Chung, Evolution of micro-deformation in inner-selective thin film composite hollow fiber membranes and its implications for osmotic power generation, Journal of Membrane Science, 516 (2016) 104-112.
[126] Z.L. Cheng, X. Li, Y. Feng, C.F. Wan, T.-S. Chung, Tuning water content in polymer dopes to boost the performance of outer-selective thin-film composite (TFC) hollow fiber membranes for osmotic power generation, Journal of Membrane Science, 524 (2017) 97-107.
[127] C.F. Wan, B. Li, T. Yang, T.-S. Chung, Design and fabrication of inner-selective thin-film composite (TFC) hollow fiber modules for pressure retarded osmosis (PRO), Separation and Purification Technology, 172 (2017) 32-42.
[128] Y. Chen, C.H. Loh, L. Zhang, L. Setiawan, Q. She, W. Fang, X. Hu, R. Wang, Module scale-up and performance evaluation of thin film composite hollow fiber membranes for pressure retarded osmosis, Journal of Membrane Science, 548 (2018) 398-407.
[129] P.G. Ingole, W. Choi, K.-H. Kim, H.-D. Jo, W.-K. Choi, J.-S. Park, H.-K. Lee, Preparation, characterization and performance evaluations of thin film composite hollow fiber membrane for energy generation, Desalination, 345 (2014) 136-145.
[130] P.G. Ingole, W. Choi, K.H. Kim, C.H. Park, W.K. Choi, H.K. Lee, Synthesis, characterization and surface modification of PES hollow fiber membrane support with polydopamine and thin film composite for energy generation, Chemical Engineering Journal, 243 (2014) 137-146.
[131] P.G. Ingole, K.H. Kim, C.H. Park, W.K. Choi, H.K. Lee, Preparation, modification and characterization of polymeric hollow fiber membranes for pressure-retarded osmosis, RSC Advances, 4 (2014) 51430-51439.
[132] G. Han, T.-S. Chung, Robust and high performance pressure retarded osmosis hollow fiber membranes for osmotic power generation, AIChE Journal, 60 (2014) 1107-1119.
[133] S.-P. Sun, T.-S. Chung, Outer-selective pressure-retarded osmosis hollow fiber membranes from vacuum-assisted interfacial polymerization for osmotic power generation, Environmental Science & Technology, 47 (2013) 13167-13174.
[134] Z.L. Cheng, X. Li, Y.D. Liu, T.-S. Chung, Robust outer-selective thin-film composite polyethersulfone hollow fiber membranes with low reverse salt flux for renewable salinity-gradient energy generation, Journal of Membrane Science, 506 (2016) 119-129.
[135] N.L. Le, N. Bettahalli, S.P. Nunes, T.-S. Chung, Outer-selective thin film composite (TFC) hollow fiber membranes for osmotic power generation, Journal of Membrane Science, 505 (2016) 157-166.
[136] F.-J. Fu, S. Zhang, S.-P. Sun, K.-Y. Wang, T.-S. Chung, POSS-containing delamination-free dual-layer hollow fiber membranes for forward osmosis and osmotic power generation, Journal of Membrane Science, 443 (2013) 144-155.
[137] W. Gai, D.L. Zhao, T.-S. Chung, Novel thin film composite hollow fiber membranes incorporated with carbon quantum dots for osmotic power generation, Journal of Membrane Science, 551 (2018) 94-

102.
[138] M.J. Park, S. Lim, R.R. Gonzales, S. Phuntsho, D.S. Han, A. Abdel-Wahab, S. Adham, H.K. Shon, Thin-film composite hollow fiber membranes incorporated with graphene oxide in polyethersulfone support layers for enhanced osmotic power density, Desalination, 464 (2019) 63-75.
[139] Y.H. Cho, S.D. Kim, J.F. Kim, H.-g. Choi, Y. Kim, S.-E. Nam, Y.-I. Park, H. Park, Tailoring the porous structure of hollow fiber membranes for osmotic power generation applications via thermally assisted nonsolvent induced phase separation, Journal of Membrane Science, 579 (2019) 329-341.
[140] R.R. Gonzales, Y. Yang, M.J. Park, T.-H. Bae, A. Abdel-Wahab, S. Phuntsho, H.K. Shon, Enhanced water permeability and osmotic power generation with sulfonate-functionalized porous polymer-incorporated thin film nanocomposite membranes, Desalination, 496 (2020) 114756-114765.
[141] F.-J. Fu, S.-P. Sun, S. Zhang, T.-S. Chung, Pressure retarded osmosis dual-layer hollow fiber membranes developed by co-casting method and ammonium persulfate (APS) treatment, Journal of Membrane Science, 469 (2014) 488-498.
[142] X. Li, T.-S. Chung, Thin-film composite P84 co-polyimide hollow fiber membranes for osmotic power generation, Applied Energy, 114 (2014) 600-610.
[143] C.F. Wan, T. Yang, W. Gai, Y.D. Lee, T.-S. Chung, Thin-film composite hollow fiber membrane with inorganic salt additives for high mechanical strength and high power density for pressure-retarded osmosis, Journal of Membrane Science, 555 (2018) 388-397.
[144] Y. Li, S. Zhao, L. Setiawan, L. Zhang, R. Wang, Integral hollow fiber membrane with chemical cross-linking for pressure retarded osmosis operated in the orientation of active layer facing feed solution, Journal of Membrane Science, 550 (2018) 163-172.
[145] R. Patel, W.S. Chi, S.H. Ahn, C.H. Park, H.-K. Lee, J.H. Kim, Synthesis of poly(vinyl chloride)-g-poly(3-sulfopropyl methacrylate) graft copolymers and their use in pressure retarded osmosis (PRO) membranes, Chemical Engineering Journal, 247 (2014) 1-8.
[146] X. Tong, X. Wang, S. Liu, H. Gao, C. Xu, J. Crittenden, Y. Chen, A freestanding graphene oxide membrane for efficiently harvesting salinity gradient power, Carbon, 138 (2018) 410-418.
[147] H. Gao, W. Chen, C. Xu, S. Liu, X. Tong, Y. Chen, Two-dimensional Ti3C2Tx MXene/GO hybrid membranes for highly efficient osmotic power generation, Environmental Science & Technology, 54 (2020) 2931-2940.
[148] Q. She, D. Hou, J. Liu, K.H. Tan, C.Y. Tang, Effect of feed spacer induced membrane deformation on the performance of pressure retarded osmosis (PRO): Implications for PRO process operation, Journal of Membrane Science, 445 (2013) 170-182.
[149] Y.C. Kim, M. Elimelech, Adverse impact of feed channel spacers on the performance of pressure retarded osmosis, Environmental Science & Technology, 46 (2012) 4673-4681.
[150] A.P. Straub, S. Lin, M. Elimelech, Module-scale analysis of pressure retarded osmosis: Performance limitations and implications for full-scale operation, Environmental Science & Technology, 48 (2014) 12435-12444.
[151] Y.C. Kim, Y. Kim, D. Oh, K.H. Lee, Experimental investigation of a spiral-wound pressure-

retarded osmosis membrane module for osmotic power generation, Environmental Science & Technology, 47 (2013) 2966-2973.
[152] J. Schwinge, P.R. Neal, D.E. Wiley, D.F. Fletcher, A.G. Fane, Spiral wound modules and spacers: Review and analysis, Journal of Membrane Science, 242 (2004) 129-153.
[153] M. Kishimoto, Y. Tanaka, M. Yasukawa, S. Goda, M. Higa, H. Matsuyama, Optimization of pressure-retarded osmosis with hollow-fiber membrane modules by numerical simulation, Industrial & Engineering Chemistry Research, 58 (2019) 6687-6695.
[154] M. Higa, D. Shigefuji, M. Shibuya, S. Izumikawa, Y. Ikebe, M. Yasukawa, N. Endo, A. Tanioka, Experimental study of a hollow fiber membrane module in pressure-retarded osmosis: Module performance comparison with volumetric-based power outputs, Desalination, 420 (2017) 45-53.
[155] Y. Chen, A.A. Alanezi, J. Zhou, A. Altaee, M.H. Shaheed, Optimization of module pressure retarded osmosis membrane for maximum energy extraction, Journal of Water Process Engineering, 32 (2019) 100935.
[156] J.Y. Xiong, D.J. Cai, Q.Y. Chong, S.H. Lee, T.-S. Chung, Osmotic power generation by inner selective hollow fiber membranes: An investigation of thermodynamics, mass transfer, and module scale modelling, Journal of Membrane Science, 526 (2017) 417-428.
[157] J. Ju, Y. Choi, S. Lee, Y.-G. Park, Comparison of different pretreatment methods for pressure retarded osmosis (PRO) membrane in bench-scale and pilot-scale systems, Desalination, 496 (2020) 114528-114540.
[158] D. Attarde, M. Jain, K. Chaudhary, S.K. Gupta, Osmotically driven membrane processes by using a spiral wound module — Modeling, experimentation and numerical parameter estimation, Desalination, 361 (2015) 81-94.
[159] S. Lee, Y.C. Kim, S.-J. Park, S.-K. Lee, H.-C. Choi, Experiment and modeling for performance of a spiral-wound pressure-retarded osmosis membrane module, Desalination and Water Treatment, 57 (2016) 10101-10110.
[160] M. Kurihara, H. Sakai, A. Tanioka, H. Tomioka, Role of pressure-retarded osmosis (PRO) in the mega-ton water project, Desalination and Water Treatment, 57 (2016) 26518-26528.
[161] K. Saito, M. Irie, S. Zaitsu, H. Sakai, H. Hayashi, A. Tanioka, Power generation with salinity gradient by pressure retarded osmosis using concentrated brine from SWRO system and treated sewage as pure water, Desalination and Water Treatment, 41 (2012) 114-121.
[162] H.S. Chae, M.Y. Kim, H. Park, J. Seo, J.S. Lim, H.J. Kim, Modeling and simulation studies analyzing the pressure-retarded osmosis (PRO) and PRO-hybridized processes, Energies, 12 (2019).
[163] A. Altaee, N. Hilal, Dual-stage forward osmosis/pressure retarded osmosis process for hypersaline solutions and fracking wastewater treatment, Desalination, 350 (2014) 79-85.
[164] S.H. Chae, J. Seo, J. Kim, Y.M. Kim, J.H. Kim, A simulation study with a new performance index for pressure-retarded osmosis processes hybridized with seawater reverse osmosis and membrane distillation, Desalination, 444 (2018) 118-128.
[165] J.L. Prante, J.A. Ruskowitz, A.E. Childress, A. Achilli, RO-PRO desalination: An integrated low-

energy approach to seawater desalination, Applied Energy, 120 (2014) 104-114.
[166] A. Tanioka, Preface to the special issue on “Pressure Retarded Osmosis in Megaton Water System Project”, Desalination, 389 (2016) 15-17.
[167] A. Tanioka, M. Kurihara, H. Sakai, Megaton Water System: High Salinity Pressure Retarded Osmosis, in: S. Sarp, N. Hilal (Eds.) Membrane-Based Salinity Gradient Processes for Water Treatment and Power Generation, Elsevier, 2018.
[168] J. Kim, K. Jeong, M.J. Park, H.K. Shon, J.H. Kim, Recent advances in osmotic energy generation via pressure-retarded osmosis (PRO): A review, Energies, 8 (2015) 11821-11845.
[169] S. Lee, S.-H. Kim, Y.-G. Park, High-Salinity Pressure Retarded Osmosis Using Seawater Reverse Osmosis Brine, in: S. Sarp, N. Hilal (Eds.) Membrane-Based Salinity Gradient Processes for Water Treatment and Power Generation, Elsevier, 2018.
[170] J. Kim, M. Park, S.A. Snyder, J.H. Kim, Reverse osmosis (RO) and pressure retarded osmosis (PRO) hybrid processes: Model-based scenario study, Desalination, 322 (2013) 121-130.
[171] A. Achilli, J.L. Prante, N.T. Hancock, E.B. Maxwell, A.E. Childress, Experimental results from RO-PRO: A next generation system for low-energy desalination, Environmental Science & Technology, 48 (2014) 6437-6443.
[172] A. Altaee, G. Zaragoza, A. Sharif, Pressure retarded osmosis for power generation and seawater desalination: Performance analysis, Desalination, 344 (2014) 108-115.
[173] C.F. Wan, T.-S. Chung, Energy recovery by pressure retarded osmosis (PRO) in SWRO–PRO integrated processes, Applied Energy, 162 (2016) 687-698.
[174] E. Bargiacchi, F. Orciuolo, L. Ferrari, U. Desideri, Use of pressure-retarded-osmosis to reduce reverse osmosis energy consumption by exploiting hypersaline flows, Energy, 211 (2020) 118969.
[175] C.F. Wan, T.-S. Chung, Maximize the operating profit of a SWRO-PRO integrated process for optimal water production and energy recovery, Renewable Energy, 94 (2016) 304-313.
[176] N. Sawaki, C.-L. Chen, Cost evaluation for a two-staged reverse osmosis and pressure retarded osmosis desalination process, Desalination, 497 (2021) 114767.
[177] K. Touati, J. Salamanca, F. Tadeo, H. Elfil, Energy recovery from two-stage SWRO plant using PRO without external freshwater feed stream: Theoretical analysis, Renewable Energy, 105 (2017) 84-95.
[178] K. Touati, H.S. Usman, C.N. Mulligan, M.S. Rahaman, Energetic and economic feasibility of a combined membrane-based process for sustainable water and energy systems, Applied Energy, 264 (2020) 114699.
[179] Z.L. Cheng, X. Li, T.-S. Chung, The forward osmosis-pressure retarded osmosis (FO-PRO) hybrid system: A new process to mitigate membrane fouling for sustainable osmotic power generation, Journal of Membrane Science, 559 (2018) 63-74.
[180] M. Meng, S. Liu, X. Wang, Pressure retarded osmosis coupled with activated sludge process for wastewater treatment: Performance and fouling behaviors, Bioresource Technology, 307 (2020) 123224.
[181] G. Han, J. Zuo, C. Wan, T.-S. Chung, Hybrid pressure retarded osmosis-membrane distillation

(PRO-MD) process for osmotic power and clean water generation, Environmental Science: Water Research & Technology, 1 (2015) 507-515.
[182] J.-G. Lee, Y.-D. Kim, S.-M. Shim, B.-G. Im, W.-S. Kim, Numerical study of a hybrid multi-stage vacuum membrane distillation and pressure-retarded osmosis system, Desalination, 363 (2015) 82-91.
[183] Y. Wang, S. Luo, J. Guo, M. Liu, J. Wang, J. Yan, T. Luo, LIS-PRO: A new concept of power generation from low temperature heat using liquid-phase ion-stripping-induced salinity gradient, Energy, 200 (2020) 117593.
[184] S. Loeb, Method and apparatus for generating power utilizing pressure-retarded-osmosis, in, Ben Gurion University of the Negev Research and Development Authority Ltd., United States, 1975.
[185] K.L. Hickenbottom, J. Vanneste, T.Y. Cath, Assessment of alternative draw solutions for optimized performance of a closed-loop osmotic heat engine, Journal of Membrane Science, 504 (2016) 162-175.
[186] R.L. McGinnis, J.R. McCutcheon, M. Elimelech, A novel ammonia–carbon dioxide osmotic heat engine for power generation, Journal of Membrane Science, 305 (2007) 13-19.
[187] E. Shaulsky, C. Boo, S. Lin, M. Elimelech, Membrane-based osmotic heat engine with organic solvent for enhanced power generation from low-grade heat, Environmental Science & Technology, 49 (2015) 5820-5827.
[188] S. Lin, N.Y. Yip, T.Y. Cath, C.O. Osuji, M. Elimelech, Hybrid pressure retarded osmosis–membrane distillation system for power generation from low-grade heat: Thermodynamic analysis and energy efficiency, Environmental Science & Technology, 48 (2014) 5306-5313.
[189] A. Altaee, P. Palenzuela, G. Zaragoza, A.A. AlAnezi, Single and dual stage closed-loop pressure retarded osmosis for power generation: Feasibility and performance, Applied Energy, 191 (2017) 328-345.
[190] A. Altaee, A. Sharif, G. Zaragoza, N. Hilal, Dual stage PRO process for power generation from different feed resources, Desalination, 352 (2014) 118-127.
[191] W. He, Y. Wang, M.H. Shaheed, Enhanced energy generation and membrane performance by two-stage pressure retarded osmosis (PRO), Desalination, 359 (2015) 186-199.
[192] F.J. Arias, S. De Las Heras, Pool pressure-retarded osmosis, International Journal of Energy Research, 44 (2020) 7841-7845.
[193] B. Blankert, Y. Kim, H. Vrouwenvelder, N. Ghaffour, Facultative hybrid RO-PRO concept to improve economic performance of PRO: Feasibility and maximizing efficiency, Desalination, 478 (2020) 114268.
[194] S. Adham, A. Hussain, J. Minier-Matar, A. Janson, R. Sharma, Membrane applications and opportunities for water management in the oil & gas industry, Desalination, 440 (2018) 2-17.
[195] A. Janson, D. Dardor, M. Al Maas, J. Minier-Matar, A. Abdel-Wahab, S. Adham, Pressure-retarded osmosis for enhanced oil recovery, Desalination, 491 (2020) 114568.
[196] H.T. Madsen, T. Bruun Hansen, T. Nakao, S. Goda, E.G. Søgaard, Combined geothermal heat and pressure retarded osmosis as a new green power system, Energy Conversion and Management, 226

(2020) 113504.
[197] C. Lee, S.H. Chae, E. Yang, S. Kim, J.H. Kim, I.S. Kim, A comprehensive review of the feasibility of pressure retarded osmosis: Recent technological advances and industrial efforts towards commercialization, Desalination, 491 (2020) 114501.
[198] P. Stenzel, H.-J. Wagner, Osmotic power plants: Potential analysis and site criteria, in: 3rd International Conference on Ocean Energy, Bilbao, Spain, 2010.
[199] A. Altaee, A. Cipolina, Modelling and optimization of modular system for power generation from a salinity gradient, Renewable Energy, 141 (2019) 139-147.